IAIK

SCIENCE ▪ PASSION ▪ TECHNOLOGY

TU Graz

Peter Julius Waldert

Secure Classification as a Service

Levelled Homomorphic, Post-Quantum Secure Machine Learning Inference
based on the CKKS Encryption Scheme

BACHELOR'S THESIS

Bachelor's degree programmes:
Physics and *Information & Computer Engineering*

Supervisor

Dipl.-Ing. Roman Walch

Institute of Applied Information Processing and Communications (IAIK)
Graz University of Technology

Graz, July 2022

Abstract

The rapid developments in quantum computation affect cryptography as it is used today. With a sufficiently powerful quantum computer, most digital communication could be decrypted in polynomial time by an eavesdropping party with access to such a potent utility, posing a major problem to the worldwide community. Lattice-based cryptographic schemes aim to mitigate this, while including many further advantages, which will be the main topic of this thesis.

With technological advancements in machine learning, problems long thought to be impossible can now be solved by complicated and resource-intensive neural network structures. Machine learning undoubtedly holds many new possibilities, especially in medicine, although large datasets are especially scarce in this area. Privacy-Preserving Machine Learning (PPML) is an emerging field in data science that focusses on leveraging such highly private data anyway, without ever actually seeing it. The techniques behind this are homomorphic encryption schemes, two of which this thesis will discuss in detail.

To demonstrate the possibilities of these homomorphic cryptosystems applied to machine learning inference, a web-based demonstrator for the classification of handwritten digits was developed (confer figure 1.1). The backend server is written in C++, using the Microsoft SEAL homomorphic encryption library. This work starts by introducing the necessary mathematical background, motivating the definitions of the BFV and CKKS encryption schemes in the following chapter and describing the basics of machine learning along the way. The quantum-mechanical principles and implications of Shor's algorithm are discussed, further inciting the need for studying the hardness of the LWE-based cryptosystems. The final chapters then focus on implementation aspects, the analysis of obtained results and performance benchmarks.

Keywords: FHE, ML, Image Classification, Neural Network, Private AI, PPML, Confidential Computing, Post-Quantum Security

Technologies: Microsoft SEAL (C++, NodeJS), Tensorflow Keras, Numpy, xtensor, Docker, msgpack, React, Materialize, Nginx

Languages: C++, Python, JavaScript

Contents

Chapter 1

Introduction

The most well-known and widely used asymmetric ('public-key') cryptographic scheme, published by the trio Rivest-Shamir-Adleman in 1977 and known as RSA, is based on the hardness assumption of the integer factorisation problem, factorising a large 2-composite number into its two prime factors p and q is believed to be hard (R. L. Rivest, Shamir and L. M. Adleman 1983). As of today, this factorisation problem has not been proven to be in the Non-deterministic Polynomial time (NP) complexity class, yet it is suspected that it might indeed be NP-complete (i.e. NP-hard while still being in NP) when modelled using a traditional Turing machine. Since the advent of quantum computation, this situation changed as a whole with Peter Shor's algorithm (Shor 1997), threatening the security of many cryptosystems, for instance Rivest-Shamir-Adleman (RSA) which is still widely used today despite its known problems.

As it stands, lattice-based cryptography presents a solution to a politically and socially problematic situation in which few parties world-wide, with access to a sufficiently powerful quantum computer, may be able to decrypt most of today's digital communication. Lattice Cryptography is based on other mathematical problems, shown to be sufficiently hard on quantum computers and traditional ones alike, most notably LWE (Regev 2005) which this thesis will discuss in detail.

Many new cryptosystems have been developed on top of LWE, two of which this following thesis will focus on specifically: BFV and CKKS; whose security is still unaffected by efficient quantum algorithms. Yet, it is not only their security prospect that makes these encryption schemes attractive, but primarily their defining homomorphic property which allows for computations on the encrypted data. A *fully* homomorphic encryption scheme was first introduced by Craig Gentry in 2009, using a bootstrapping approach (Gentry 2009). The *levelled* homomorphic Brakerski-Gentry-Vaikuntanathan (BGV) encryption scheme is implemented in *Microsoft SEAL 4.0* 2022 and allows for integer arithmetic, up to a few multiplication 'levels' deep (Brakerski, Gentry and Vaikuntanathan 2012). The Brakerski-Fan-Vercauteren (BFV) scheme (Fan and Vercauteren 2012; Brakerski 2012) is highly similar and described in a bit more detail in section 3.3. And finally, building upon concepts introduced in the former, the Cheon-Kim-Kim-Song (CKKS) scheme (Cheon et al. 2017) allows for approximative floating-point arithmetic that finally facilitates machine-learning applications.

Machine Learning allows a computer to 'learn' from specifically structured data using linear regression or similar methods, and to apply this 'knowledge' to new, unknown inputs. In its simplest form, or even using a multi-layered neural network, this only requires two different operations on numbers (or even better, vectors): addition and multiplication. Using one of the

Homomorphic Encryption (HE) schemes mentioned above and described in chapter 3, both are given and PPML applications are born!

The present thesis not only focusses on theoretical remarks but also includes a publicly available implementation of an HE classification server written in C++, based on the Homomorphic Encryption library Simple Encrypted Arithmetic Library (SEAL) developed by Microsoft Research (*Microsoft SEAL 4.0* 2022), and a compact graphical user interface to interact with. A screenshot of the main functionality is displayed in figure 1.1.

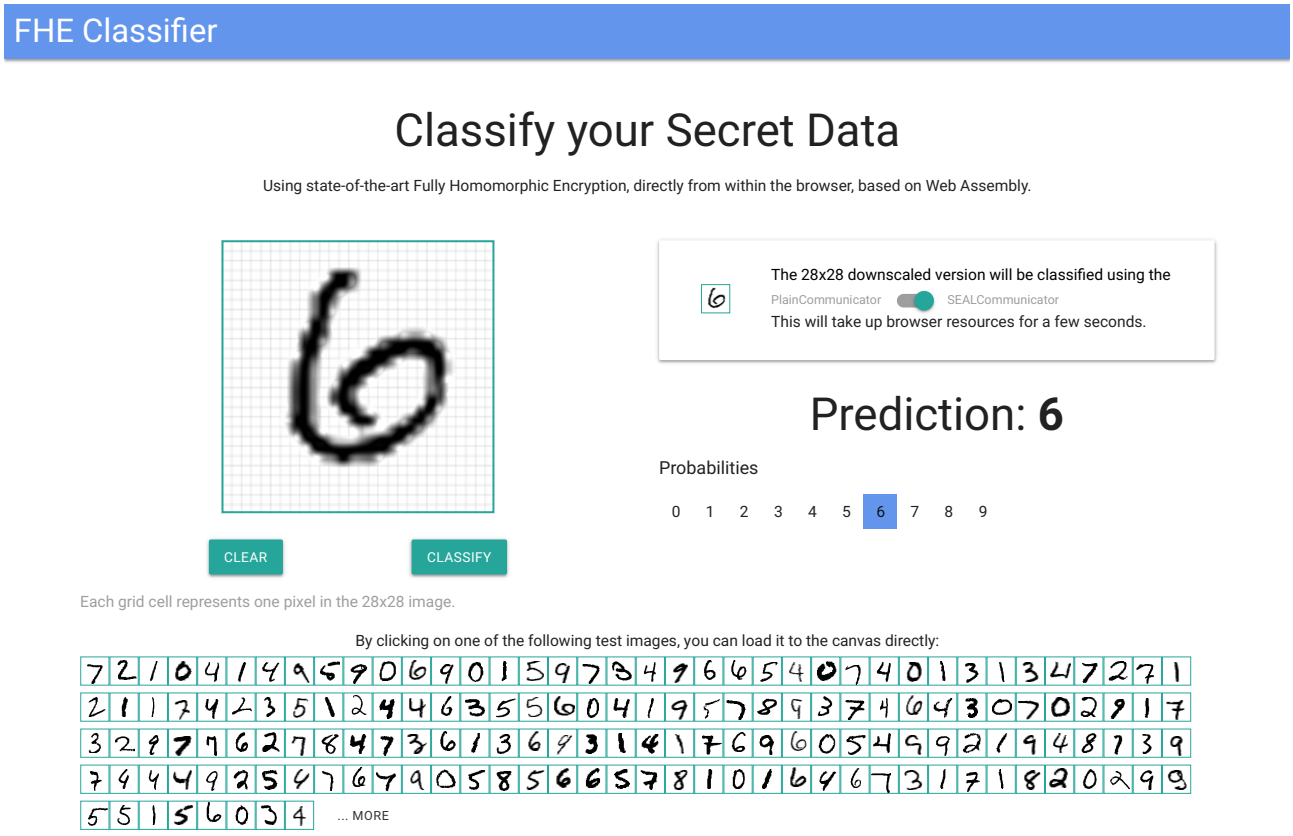

Figure 1.1: The user interface of the demonstrator: users can draw a digit by hand, select one of two communication means (plain or encrypted) and finally let the server handle the classification to obtain a prediction (including a visual of associated probabilities).

The following chapter 2 and chapter 3 aim to introduce most of the necessary theory to understand the HE schemes used in practice today, as well as the simple machine learning approaches involved in securely classifying images as a service.

Chapter 4 then focusses on the concrete system at hand, how the classification of handwritten digits (using the MNIST dataset) works in detail and what challenges arise when dealing with a system which acts not only on plain, but also encrypted data. Chapter 5 analyses the neural network performance in terms of its accuracy, digit-wise precision and recall, documents benchmarks of runtime, message size and accuracy and finally includes a visualisation of the ciphertext (containing all information about the original image).

Chapter 2

Background

The discussion of the HE schemes following in chapter 3 requires some mathematical background that will be introduced here, aiming for a consistent overview rather than full completeness. The last two sections 2.3 and 2.4 introduce some background on Machine Learning and provide an outlook on Quantum Computation and why it affects cryptography today.

Notational Conventions: Let $\mathbb{N}$ denote the natural numbers without 0. For a probability distribution χ over a set R, let sampling a value $x \in R$ from the probability distribution be denoted by $x \leftarrow \chi$. For $a \in \mathbb{R}$ a real number, denote rounding down (floor) a by $\lfloor a \rfloor \in \mathbb{Z}$, rounding up (ceil) by $\lceil a \rceil \in \mathbb{Z}$ and rounding to the nearest integer by $\lfloor a \rceil \in \mathbb{Z}$. Let $[a]_q := a \mod q$ denote the positive remainder when dividing a by q.

2.1 Polynomial Rings and Modular Arithmetic

As the algebraic structure underlying almost every single symbol following in the next chapters, we recall the definition of a ring:

2.1.1 Definition: Ring

A tuple $(R, +, \cdot)$ consisting of a set R, an addition operation $+$ and a multiplication operation $\cdot$ is referred to as a ring, given that it satisfies the following *ring axioms*:

- Addition is closed: $a + b \in R \quad \forall a, b \in R$.
- Addition is commutative: $a + b = b + a \quad \forall a, b \in R$.
- Addition is associative: $(a + b) + c = a + (b + c) \quad \forall a, b, c \in R$.
- There exists an element $0 \in R$ such that $a + 0 = a \quad \forall a \in R$.
- An additive inverse $-a$ of each element a in R exists, such that $a + (-a) = 0$.
- Multiplication is associative: $(a \cdot b) \cdot c = a \cdot (b \cdot c) \quad \forall a, b, c \in R$.
- Multiplication is closed: $a \cdot b \in R \quad \forall a, b \in R$.
- There exists an element $1 \in R$, referred to as the identity element, or multiplicative identity of R, such that $a \cdot 1 = a \quad \forall a \in R$.
- Multiplication $\cdot$ is distributive w.r.t. addition $+$,
  i.e. $a \cdot (b + c) = (a \cdot b) + (a \cdot c) \quad \forall a, b, c \in R$ from the left and
  i.e. $(b + c) \cdot a = (b \cdot a) + (c \cdot a) \quad \forall a, b, c \in R$ from the right.

If multiplication is additionally commutative, we refer to the ring as *commutative*:

- Multiplication is commutative: $a \cdot b = b \cdot a \quad \forall a, b \in R$.

Acting as the logical extension of a group, a ring can be considered the intermediary step towards a field (which also defines subtraction and division). Recall that the first 5 properties can be summarised as $(R, +)$ forming an Abelian group. An example of a ring would be the integers themselves, or the integers modulo q: $\mathbb{Z}/q\mathbb{Z}$, sometimes also denoted as $\mathbb{Z}_q$.

Given two groups $(G, +)$ and a subgroup $(N, +)$, we can construct another group G/N as follows, referred to as a quotient group or factor group:

2.1.2 Definition: Quotient Group / Ring

A quotient group $(G/N, +)$ (pronounced 'G mod N') over the original group G and a normal subgroup N of G with a standard element operation $+$ can be defined using the left cosets

$$g + N := \{g + n \,|\, n \in N\} \subseteq G$$

of N in G. The corresponding set G/N is defined as

$$G/N := \{g + N \,|\, g \in G\}$$

whereas the standard operation $+ : G/N \times G/N \mapsto G/N$ can be extended from the original group G as follows ($g, h \in G$):

$$(g + N) + (h + N) := (g + h)N$$

The quotient set G/N can therefore be identified as the set of all possible left cosets $g + N$ that in union reconstruct the original group G.

As a highly relevant structure to cryptography and a great example of a quotient group, we would like to consider the ring of integers modulo a given modulus $q \in \mathbb{N}$.

2.1.1 Lemma: Ring of Integers Modulo q: $\mathbb{Z}/q\mathbb{Z}$

Using equivalence classes $\overline{x}_q$ modulo q referred to as congruence classes, define the commutative quotient ring of integers modulo q as $(\mathbb{Z}/q\mathbb{Z}, +, \cdot)$ with two operations $+$ and $\cdot$ and

$$\mathbb{Z}/q\mathbb{Z} = \{\overline{x}_q \,|\, x \in \mathbb{Z}, 0 \leq x < q\}$$

where $q\mathbb{Z} = \{qx \,|\, x \in \mathbb{Z}\} \triangleleft \mathbb{Z}$ (where $\triangleleft$ refers to the left being a subgroup of the right) denotes the q^{th} multiplicative coset[a] of the integers and

$$\overline{x}_q = \{y \equiv x \mod q \,|\, y \in \mathbb{Z}\}$$

is the set of all multiples of q with remainder x. Note that many operations that resulting groups, rings or fields are commonly equipped with, such as addition or multiplication, propagate to an equivalent definition in the ring of integers modulo q by considering their result as a congruence class instead of it, which in turn is again an element of $\mathbb{Z}/q\mathbb{Z}$.

[a] from the left and from the right, therefore $q\mathbb{Z}$ is called a normal subgroup of $\mathbb{Z}$

This ring is of specific importance in discrete mathematics and can be regarded as a formalisation of modular arithmetic, much of which we will require at a later point in this chapter.

As a first step towards the first central result, corollary 2.1.1, we formally introduce polynomial rings and how to carry out addition and multiplication between them.

2.1.3 Definition: Polynomial Ring over $\mathbb{Z}$

On the set of all complex-valued polynomials with integer coefficients (a function space)

$$\mathbb{Z}[X] = \Big\{p : \mathbb{C} \mapsto \mathbb{C}\,, p(x) = \sum_{k=0}^{\infty} a_k x^k, a_k \in \mathbb{Z}\ \forall k \geq 0\Big\},$$

we can define a commutative ring $(\mathbb{Z}[X], +, \cdot)$ equipped with the standard addition $+$ and multiplication $\cdot$ operations (as an extension over the field $\mathbb{C}$) of polynomials.

To further elaborate on the polynomial ring operations:

- In their coefficient representations $\boldsymbol{p} = (p_j)_{j\in\mathbb{N}} = (p_0, p_1, p_2, ...)$ (which are sequences) and $\boldsymbol{q} = (q_j)_{j\in\mathbb{N}} = (q_0, q_1, q_2, ...)$, an addition of two polynomials $p, q \in \mathbb{Z}[X]$ is equivalent to the element-wise addition of their coefficient sequences

$$\begin{aligned}(p+q)(X) &= \sum_{k=0}^{\infty} p_k X^k + \sum_{k=0}^{\infty} q_k X^k = \sum_{k=0}^{\infty} (p_k + q_k) X^k \\ &= \langle (\boldsymbol{p} + \boldsymbol{q}), \{X^0, X^1, X^2, ...\}^T \rangle\end{aligned}$$

  which indeed satisfies the additive ring axioms (cf. definition 2.1.1) due to the existing structure of the underlying field $\mathbb{C}$.

- The multiplication operation can be defined using a discrete convolution of the coefficient vectors

$$r(X) = (p \cdot q)(X) = (\sum_{k=0}^{\infty} p_k X^k) \cdot (\sum_{l=0}^{\infty} q_l X^l) = \sum_{k=0}^{\infty} \sum_{l=0}^{\infty} p_k q_l X^{k+l} = \sum_{k=0}^{\infty} r_k X^k$$

  with the arising coefficients $(r_k)_{k\in\mathbb{N}}$ determined by the discrete convolution

$$r_k = \sum_{l=0}^{k} p_l q_{k-l} \ \Leftrightarrow\ \boldsymbol{r} = \boldsymbol{p} * \boldsymbol{q}$$

  in this context also referred to as the Cauchy-product. Therefore,

$$(p \cdot q)(X) = \langle (\boldsymbol{p} * \boldsymbol{q}), \{X^0, X^1, X^2, ...\}^T \rangle.$$

  Again, this generally applicable approach satisfies the multiplicative ring axioms and even satisfies commutativity due to the existing structure of the underlying field $\mathbb{C}$ and the symmetry of convolutions.

Where $\langle \cdot, \cdot \rangle$ denotes the dot (scalar) product between two vectors.

Polynomials with degree ≥ 1 over the complex numbers can always be factorised using their roots due to the fundamental theorem of algebra. Polynomials over the integers however, cannot always be factorised further, yielding the definition of an irreducible polynomial.

2.1.4 Definition: Irreducible Polynomials

A polynomial is called irreducible if and only if (iff) it cannot be written as a product of other polynomials *while staying in the same coefficient space*.

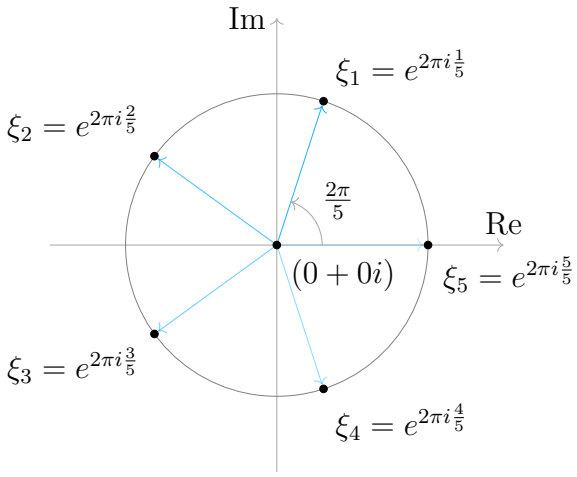

Figure 2.1: The 5^{th} roots of unity visualised on the complex plane. Obviously, they all lie on the unit circle $|z| = 1$, motivating the name of cyclotomic, 'circle-cutting', polynomials, whose roots cut the unit circle into multiple sectors.

2.1.1 Cyclotomic Polynomials

Due to their interesting structure and efficient computability, in the schemes introduced in the following chapter, certain polynomials (corollary 2.1.1) are chosen as representations of plaintexts and ciphertexts. An important concept is that of cyclotomic ('circle-cutting') polynomials, which we will discuss in a bit more detail here.

An important polynomial is

$$p : \mathbb{C} \mapsto \mathbb{C},\ p(x) = x^n - 1\,.$$

Its roots, found by solving $p(\xi) = 0$ for ξ, yielding $\xi^n = 1 \leftrightarrow \xi_k = \sqrt[n]{1}$ are referred to as the n^{th} roots of unity, of which there are multiple for each $n \in \mathbb{N}$.

2.1.2 Lemma: The n^{th} roots of unity

For some integer $n \in \mathbb{N}$, the n complex roots $\xi_1, \xi_2, ..., \xi_n \in \mathbb{C}$ of unity can be found as

$$\xi_k = e^{2\pi i \frac{k}{n}} \quad k \in \{1, 2, ..., n\}$$

with i being the imaginary unit. Confer figure 2.1. Using Euler's identity, their real and imaginary components can be explicitly found as $\xi_k = \cos\left(2\pi\frac{k}{n}\right) + i\sin\left(2\pi\frac{k}{n}\right)$.
An n^{th} root of unity y is referred to as *primitive*, iff there exists no $m < n$ for which that root y is also an m^{th} root of unity, i.e. $y^m \neq 1$. An equivalent indicator of a primitive root is $\gcd(m, n) = 1$, referring to the greatest common divisor between m and n which is 1 iff they are mutually prime.

Due to the fact that for any $k, l \in \mathbb{Z}$, their product $\xi_k \cdot x_l$ is also a root of unity, and $\xi_{k+jn} = \xi_k\ \forall j \in \mathbb{Z}$, they clearly comprise a cyclic Abelian group over the complex numbers $\mathbb{C}$ under multiplication with (for instance) the first root $\xi_1 = e^{2\pi i \frac{1}{n}}$ as its generator.

2.1.5 Definition: Cyclotomic Polynomial

Given the n^{th} roots of unity $\{\xi_k\}$, we can define the n^{th} cyclotomic polynomial $\Phi_n \in \mathbb{Z}[X]$ as the product over all primitive roots of unity

$$\Phi_n(x) = \prod_{\substack{k=1 \\ \xi_k \text{primitive}}}^{n} (x - \xi_k)\,.$$

It is unique for each given $n \in \mathbb{N}$.

The number of primitive roots of unity is given by $\varphi(n)$, denoting Euler's totient function which counts the natural numbers m less than n who do not share a common divisor $\neq 1$, i.e. $\gcd(m, n) = 1$. $\varphi(n)$ therefore also counts the number of primitive roots of unity for n, consequently also yielding the degree of the n^{th} cyclotomic polynomial.

An important aspect of cyclotomic polynomials is that they are irreducible over their coefficient space, the integers $\mathbb{Z}$.

2.1.1 Remark: Irreducibility of Cyclotomic Polynomials

Cyclotomic polynomials are always irreducible.

This enables us to *uniquely* define a quotient ring with cyclotomic polynomials as moduli, later. In theory, there are multiple equivalent definitions of said ring, but by convention we choose the cyclotomic polynomial because it cannot be simplified further. The proof for remark 2.1.1 is quite cumbersome, but can be found in Serge 2002.

2.1.1 Theorem: $2^{k\text{th}}$ Cyclotomic Polynomial

The N^{th} cyclotomic polynomial, where $M = 2N = 2^k$ $(k \in \mathbb{N})$ is a power of 2, can be identified as

$$\Phi_M(x) = x^N + 1\,.$$

Its degree is N, consistent with $\varphi(2^k) = 2^{k-1}\ \forall k \in \mathbb{N}$.

Find a short but illustrative proof of theorem 2.1.1 in appendix A.1.

2.1.6 Definition: Ring of Polynomials of highest degree $N-1$

For a power-of-2 N, one can construct the quotient ring $(R, +, \cdot)$ as

$$R = \mathbb{Z}[X]/(X^N + 1)$$

where $(X^N + 1)$ denotes the set of all polynomial multiples of the polynomial $p \in \mathbb{Z}[X], p(x) = x^N + 1$, so

$$(X^N + 1) = \{q : \mathbb{C} \mapsto \mathbb{C},\ q(x) = r(x) \cdot (x^N + 1) \mid r \in \mathbb{Z}[X]\}.$$

The elements of R are then polynomials with integer coefficients of maximum degree $N - 1$.

If N is a power of 2, according to theorem 2.1.1,

$$R = \mathbb{Z}[X]/\Phi_d(X) = \mathbb{Z}[X]/(X^N + 1)$$

is the set of integer-coefficient polynomials reduced modulo $\Phi_d(X)$, the d^{th} cyclotomic polynomial with $N = \varphi(d) = \frac{d}{2}$. Since every cyclotomic polynomial is irreducible, this is a unique representation of R without any possible further simplifications. Therefore, in the following we will focus on power-of-2 cyclotomic polynomials, which turn out to be even more useful when defining FFT-optimized operations on them.

As promised above, we will require lemma 2.1.1 for the fundamental structure underlying the HE schemes described in the next chapter, defining ourselves a ring with coefficients in said quotient ring $\mathbb{Z}/q\mathbb{Z}$.

2.1.1 Corollary: Polynomial Ring modulo q

Further modifying $R = \mathbb{Z}[X]/(X^N + 1)$ for N a power of 2 to only take coefficients mod q, we obtain two equivalent definitions for the same ring:

$$R_q = R/qR = (\mathbb{Z}/q\mathbb{Z})[X]/(X^N + 1)$$

which contains polynomials with integer coefficients modulo q of degree $N - 1$. Explicitly stated, the set can be written as:

$$R/qR = \{p : \mathbb{C} \mapsto \mathbb{C},\ p(x) = \sum_{k=0}^{N-1} a_k x^k \mid a_k \in \mathbb{Z}/q\mathbb{Z}\}$$

This bounded polynomial ring is central to understanding objects in the next chapter and corollary 2.1.1 can be regarded as the central result of this section.

2.2 Lattice Cryptography

Lattice-based cryptography takes a different approach to encryption than classical factorisation or the discrete logarithm problem, as it is based on different hardness assumptions, namely ones on lattice problems. The goal of any mathematical encryption scheme is to leave a potential attacker with a computationally hard, at best infeasible, problem to solve when attempting to decrypt messages without a secret key. This section will start with three basic problems, SVP, GapSVP and SIS and move on to Learning With Errors (LWE) and Learning With Errors on Rings (RLWE). To illustrate the connection of these problems to lattices, we take a closer look at them before considering further details of LWE. Most notably, lattice problems are conjectured to be secure against quantum computers (Corrigan-Gibbs, S. Kim and Wu 2018).

2.2.1 Definition: Lattice

A lattice $(\mathcal{L}, +, \cdot)$ is a vector field over the integers $(\mathbb{Z}, +, \cdot)$, defined using a set of n basis vectors $\boldsymbol{b_1}, \boldsymbol{b_2}, ..., \boldsymbol{b_n} \in \mathbb{R}^n$, that can be introduced as a set

$$\mathcal{L} = \left\{ \sum_{i=1}^{n} c_i \boldsymbol{b}_i \,\middle|\, c \in \mathbb{Z} \right\} \subseteq \mathbb{R}^n$$

equipped with at least vector addition $+ : \mathcal{L} \times \mathcal{L} \mapsto \mathcal{L}$ and scalar multiplication $\cdot : \mathbb{Z} \times \mathcal{L} \mapsto \mathcal{L}$. As an extension of $\mathbb{R}^n$, the Euclidean norm $||\cdot||$ is also defined and the standard Euclidean metric $d : \mathcal{L} \times \mathcal{L} \mapsto \mathbb{R}$, yielding a metric space $(\mathcal{L}, d)$, can be obtained by the norm of a vector difference, denoted $||(\cdot) - (\cdot)||$.

Lattices are a common concept appearing in many areas of mathematics and physics, related to their effective representation as data structures and also geometric intuition (cf. figure 2.2). Its *minimum distance* λ_{min} is defined as the smallest Euclidean distance between two points $\boldsymbol{p_1}, \boldsymbol{p_2} \in \mathcal{L}$

$$\lambda_{min} = \min_{\boldsymbol{p_1}, \boldsymbol{p_2} \in \mathcal{L}} d(\boldsymbol{p_1}, \boldsymbol{p_2}) = \min_{\boldsymbol{p_1}, \boldsymbol{p_2} \in \mathcal{L}} ||\boldsymbol{p_1} - \boldsymbol{p_2}|| \,,$$

which can be equivalently thought of as the minimal length of any non-zero vector in the lattice $\mathcal{L}$, because of $\mathbf{0}$ always being an element of the lattice which can be chosen as $\boldsymbol{p_1}$ and the translational symmetry between fundamental lattice volumes (or regions).

The three problems frequently showing up in cryptography are stated below, each taking a different approach in their own interesting way.

2.2.2 Definition: Shortest Vector Problem (SVP)

Given a lattice $\mathcal{L}$ constructed from n basis vectors, find the shortest non-zero lattice vector $\boldsymbol{x} \in \mathcal{L} \backslash \{\mathbf{0}\}$, i.e. find $\boldsymbol{x}$ such that $||\boldsymbol{x}|| = \lambda_{min}$ (Peikert 2016).

Based on SVP, one can construct GapSVP, an approximative version with advantages for usage in practical problems.

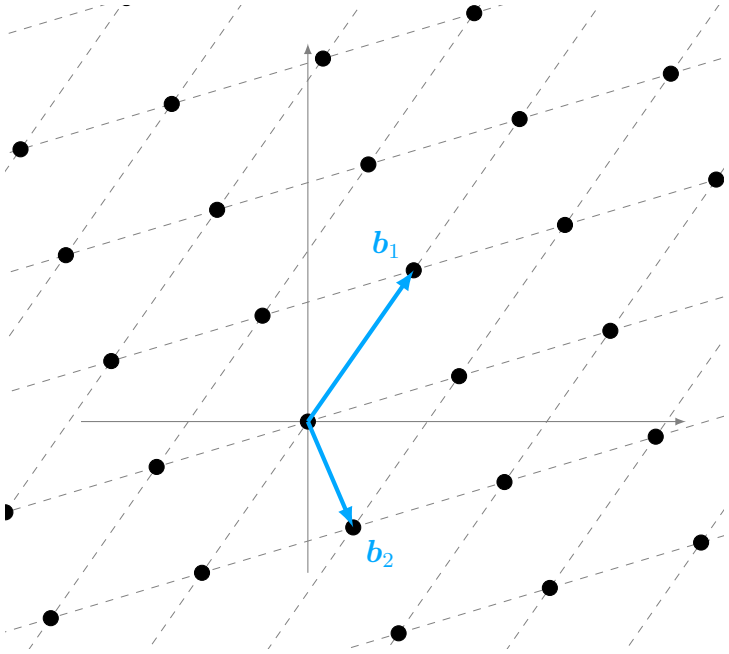

Figure 2.2: Illustration of a standard lattice $\mathcal{L}$ over the integers $\mathbb{Z}$ with two basis vectors $\boldsymbol{b}_1$ and $\boldsymbol{b}_2$ (cf. definition 2.2.1). The shortest vector problem in this case is solved by $\boldsymbol{x} = 0\boldsymbol{b}_1 \pm 1\boldsymbol{b}_2$.

2.2.3 Definition: Decisional Approximate SVP (GapSVP)

Given a lattice $\mathcal{L}$ and some pre-defined function $\gamma : \mathbb{N} \mapsto \mathbb{R}$ depending on the lattice dimension n (constant for a given $\mathcal{L}$) with $\gamma(n) \geq 1$, the decisional approximate shortest vector problem is distinguishing between $\lambda_{min} \leq 1$ and $\lambda_{min} > \gamma(n)$. For other cases, it is up to the algorithm what to return.

2.2.4 Definition: Short Integer Solution (SIS) Problem

For m given vectors $(\boldsymbol{a}_i)_{0<i\leq m} \in (\mathbb{Z}/q\mathbb{Z})^n$ that comprise the columns of a matrix $A \in (\mathbb{Z}/q\mathbb{Z})^{n\times n}$ and an upper bound β, find a solution vector $\boldsymbol{z} \in \mathbb{Z}^n \backslash \{\mathbf{0}\}$ such that

$$A\boldsymbol{z} = \mathbf{0} \quad \text{with} \quad ||\boldsymbol{z}|| \leq \beta\,.$$

Note that without the last requirement $||\boldsymbol{z}|| \leq \beta$, the Shortest Integer Solution (SIS) problem can be easily solved through Gaussian elimination or similar algorithms, however they rarely yield a short (or *the* shortest) solution. It can be shown that solving SIS is at least as hard as solving Decisional Approximate Shortest Vector Problem (GapSVP) with appropriate parameters (Ajtai 1996).

Using the above problems, multiple cryptographic primitives can be constructed due to the proven hardness that also propagates to quantum computers. Examples include collision resistant hash functions, signatures, pseudorandom functions or even Regev's public-key cryptosystem that is based on LWE, which is reduced to the other lattice problems (Peikert 2016).

2.2.1 Learning with Errors (LWE)

Next, we would like to consider LWE, a computing problem that is believed to be sufficiently hard to be used in cryptography and, most notably, is not yet solvable in linear time by a quantum algorithm (cf. section 2.4), like any other cryptographic lattice problem so far. Its hardness assumptions are related to GapSVP and were first formally proven by Regev, for which he received the 2018 Gödel price.

2.2.5 Definition: LWE-Distribution $A_{\boldsymbol{s},\chi_{error}}$

Given a prime $p \in \mathbb{N}$ and $n \in \mathbb{N}$, we choose some secret $\boldsymbol{s} \in (\mathbb{Z}/p\mathbb{Z})^n$. In order to sample a value from the LWE distribution $A_{\boldsymbol{s},\chi_{error}}$:

- Draw a random vector $a \in (\mathbb{Z}/p\mathbb{Z})^n$ from the multivariate uniform distribution with its domain in the integers up to p.
- Given another probability distribution χ_{error} over the integers modulo p, sample a scalar 'error term' $\mu \in \mathbb{Z}/p\mathbb{Z}$ from it, often also referred to as noise.
- Set $b = \boldsymbol{s} \cdot \boldsymbol{a} + \mu$, with $\cdot$ denoting the standard vector product.
- Output the pair $(\boldsymbol{a}, b) \in (\mathbb{Z}/p\mathbb{Z})^n \times (\mathbb{Z}/p\mathbb{Z})$.

The general approach useful to cryptography is to sample an element from the LWE-distribution and construct two problems out of it, *search*-LWE and *decision*-LWE.

2.2.6 Definition: LWE-Problem - Search Version

Given m independent samples $(\boldsymbol{a}_i, b_i)_{0<i\leq m}$ from $A_{\boldsymbol{s},\chi_{error}}$, find the secret $\boldsymbol{s}$.

2.2.7 Definition: LWE-Problem - Decision Version

Given m samples $(\boldsymbol{a}_i, b_i)_{0<i\leq m}$, distinguish (with non-negligible advantage) whether they were drawn from $A_{\boldsymbol{s},\chi_{error}}$ or from the uniform distribution u over $(\mathbb{Z}/p\mathbb{Z})^n \times (\mathbb{Z}/p\mathbb{Z})$.

In their above definitions, Regev showed that the two problems are equivalent.

2.2.1 Theorem: Hardness of LWE

If there exists an efficient algorithm that solves either search-LWE or decision-LWE then there exists an efficient algorithm that approximates the decision version of the shortest vector problem (GapSVP) in the worst case (Regev 2010).

He also provided a construction of a public-key cryptosystem based on them, i.e. an asymmetric cryptographic system for at least two parties that includes a public and corresponding private key.

Public-key cryptosystems are fundamentally different from symmetric systems, which only require one single key for encryption and decryption at the same time, known by all involved parties. Often times, public-key schemes (rather slow) are used to exchange keys for subsequent symmetric encryption (rather fast) of large plaintexts, for instance in the Transport Layer Security (TLS) protocol (Rescorla 2018).

2.2.2 Learning with Errors on Rings (RLWE)

Similar to definition 2.2.5, the Ring-LWE distribution is derived as follows (Lyubashevsky, Peikert and Regev 2010):

2.2.1 Corollary: RLWE-Distribution $B_{s,\chi_{error}}$

Given a quotient ring $(R/qR, +, \cdot)$, we choose some secret $s \in R/qR$. In order to sample a value from the RLWE distribution $B_{s,\chi_{error}}$:

- Uniformly randomly draw an element $a \in R/qR$
- Given another probability distribution χ_{error} over the ring elements, sample an 'error term' $\mu \in R/qR$ from it, also referred to as noise.
- Set $b = s \cdot a + \mu$, with $\cdot$ denoting the ring multiplication operation.
- Output the pair $(a, b) \in R/qR \times R/qR$.

The search and decision problems can be constructed in the same manner as for LWE:

2.2.2 Corollary: RLWE-Search Problem

Given m independent samples $(a_i, b_i)_{0<i\leq m}$ from $B_{s,\chi_{error}}$, find the secret s.

2.2.3 Corollary: RLWE-Decision Problem

Given m samples $(a_i, b_i)_{0<i\leq m}$, distinguish (with non-negligible advantage) whether they were drawn from $B_{s,\chi_{error}}$ or from the uniform distribution u over $R/qR \times R/qR$.

The main advantage of RLWE over LWE is that is conceptually similar and yet simple to formalise over an arbitrarily chosen ring $(R, +, \cdot)$ which allows for a vast amount of applications and interesting constructions.

In LWE-based cryptosystems, the public key consists of m LWE-distribution (definition 2.2.5) samples of $A_{\boldsymbol{s},\chi_{error}}$ hiding the secret $\boldsymbol{s}$. An attacker would thereby need to solve the LWE-Problem (definition 2.2.6) in order to retrieve the secret key from the public key, which is highly undesirable for a solid cryptosystem of course, but also hardly feasible with well-chosen parameters, assuming the hardness of the LWE problem (cf. theorem 2.2.1). For RLWE, the public key consists of m RLWE-distribution samples (corollary 2.2.1) which are usually smaller since they are only comprised of elements in R/qR. The size of the secret key in LWE therefore scales with $n \cdot m$, the public key with $nm + n$, while in RLWE the secret key is only a single element in R/qR and the public key only scales with $2m$. Keys are usually smaller in RLWE, depending on the choices of p, q, n and m.

Due to their similarity, RLWE samples can even be translated into equivalent LWE samples. In the case above, a straightforward way is to encode the polynomial coefficients of the RLWE public and secret key into a matrix $A \in (\mathbb{Z}/p\mathbb{Z})^{m\times n}$, vector $\boldsymbol{b} \in (\mathbb{Z}/p\mathbb{Z})^m$ and vector $\boldsymbol{s} \in (\mathbb{Z}/p\mathbb{Z})^n$ to arrive at the corresponding LWE keys. A similar approach may be chosen for the relinearisation (and possibly, Galois) keys.

This translation can be used to infer security requirements from LWE (a well-studied problem) over to RLWE to find secure parameters of the cryptosystem.

2.3 Machine Learning

Undoubtedly one of the most prevalent concepts in todays computing world, Machine Learning (ML) has shaped how computers think and how we interact with them significantly. As Shafi Goldwasser puts it, '*Machine Learning is somewhere in the intersection of Artificial Intelligence, Statistics and Theoretical Computer Science*' (Goldwasser 2018).

Within the scope of this thesis, the basics of neural networks and associated learning methods shall be covered, limited to the category of supervised learning problems (as opposed to unsupervised learning problems). Supervised learning refers to the machine *training* an algorithm to match some input data (features) with corresponding output data (targets), often related to pattern recognition. The trained algorithm can then be utilised to match fresh input data with a prediction of the targets.

A popular subset of applications to ML are classification problems, predominantly image classification, which was not as easily possible before without a human eye due to the lack of computing power. Classification problems can be formulated quickly, the goal is to computationally categorize input data (for instance, images) into a predefined set of classes (for instance, cats and dogs). The primary concept behind Machine Learning is not at all new, linear regression was already employed by Gauss and Legendre in the early 19$^{\text{th}}$ century; the term 'Neural Network' was coined by McCulloch and Pitts in 1943. Much media attention was earned in the 2000-2010 decade when larger image classification problems became feasible with the increasing computational power of modern computers, up until the advent of Deep Learning (Bishop and Nasrabadi 2007).

2.3.1 Definition: Linear Regression

Given an input vector $\boldsymbol{x} \in \mathbb{R}^n$, the goal of linear regression is to predict the value of a target $t \in \mathbb{R}$, according to some linear model M.

To illustrate the concept, we will focus on a simple learning method, namely that of gradient descent. In supervised learning problems, this technique first requires us to introduce a loss (error) function $L : \mathbb{R}^n \mapsto \mathbb{R}$, usually Mean-Squared-Error (MSE), which has comparably nice convergence properties due to its parabolic shape:

$$L(\boldsymbol{w}) = \frac{1}{2}\sum_{i=1}^{N}(t_i - \boldsymbol{w}^T\phi(\boldsymbol{x_i})) = \frac{1}{2}(\boldsymbol{t} - \Phi\boldsymbol{w})^T(\boldsymbol{t} - \Phi\boldsymbol{w})$$

where $\boldsymbol{w} \in \mathbb{R}^n$ represents the weights and $\Phi \in \mathbb{R}^{N\times(n+1)}$ is an auxiliary matrix introduced for compact notation, consisting of basis functions $\phi : \mathbb{R}^N \mapsto \mathbb{R}^N$ applied to the inputs $\boldsymbol{x_i}$, referred to as the design matrix. This approach allows for a great deal of flexibility when working with more complicated datasets, simply choosing a suitable basis often reduces the problem to a perfectly linear one, easing the fitting process. When $L(\boldsymbol{w}^*) = 0$, this means we have found the perfect weights, since our predictions exactly match the targets (labels) t_i. This is not always possible, so we aim for the minimum error between predictions and targets. In other words, our goal is to find

$$\boldsymbol{w}^* = \underset{\boldsymbol{w}\in\mathbb{R}^n}{\operatorname{argmin}}\, L(\boldsymbol{w})$$

given a dataset $\{\boldsymbol{x}_i, t_i\}$.

2.3.1 Gradient Descent

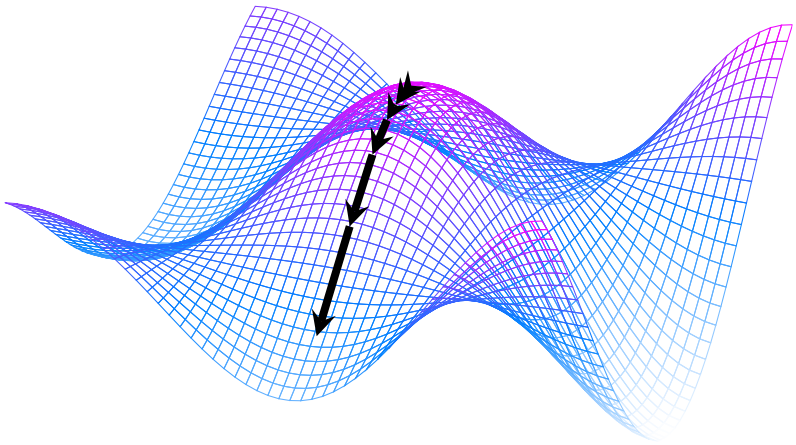

Figure 2.3: An illustration of Gradient Descent on a given loss function $L(w_x, w_y)$ in parameter space (w_x, w_y), adapted from StackExchange 2020. At each iteration, gradient descent advances in the opposite direction of the gradient $-\nabla L$ to approach a local minimum.

A common method to find such a minimum is Gradient Descent (GD), a straightforward iterative technique to find nearby minima, given a starting position $\boldsymbol{w_0}$ in 'parameter space'. In its simplest form, GD simply evaluates the *gradient* of the loss function L at the starting point $\boldsymbol{w_0}$, yielding a direction in parameter space in which the loss will increase the most at this given point. Therefore, we advance in the opposite direction given by $-\nabla L$, by a distance η. In the next iteration, our subsequent guess for the local minimum is then given by

$$\boldsymbol{w_{i+1}} = \boldsymbol{w_i} - \eta \nabla L$$

which we choose as the next starting point to repeat the process as can be seen in figure 2.3. The iteration finishes when $||\nabla L|| = 0$ and the Hessian at $\boldsymbol{w_i}$ is positive definite, indicating a proper minimum, or when a recurring loop in the iteration sequence is detected, or when the loss variation $|L(\boldsymbol{w_{i+1}}) - L(\boldsymbol{w_i})|$ deceeds a given threshold (Bishop and Nasrabadi 2007).

Note that without modification, GD is not a reliable method to find global minima, only local ones. An effective optimisation would be mixing GD with Monte-Carlo Markov Chain methods, traversing through parameter space given some probability distribution, and performing GD subsequently at multiple locations, thereby escaping the local minima's wells to possibly reach a global minimum. Another useful optimisation is to make the distance η dependent on the iteration step, causing larger jumps in the beginning and smaller ones towards the end - effectively preventing ineffective jump loops around the minimum without approaching the minimum any further.

One of the biggest advantages of Gradient Descent is its versatility, given any differentiable loss function, no matter how complicated, at least some progress can be made with GD. If the loss function has a simpler form (if it can be written as a quadratic form for instance), and to make up for numerical problems and potentially slow convergence, GD can be replaced by more sophisticated methods such as Conjugate Gradient (with convergence guarantees within a certain boundary) or by adding in momentum to the distance travelled in each GD iteration (Bishop and Nasrabadi 2007).

2.3.2 Multi-Layered Neural Networks

As the relations behind data become more and more complicated, the demand for more sophisticated modelling methods increases. Frank ROSENBLATT first implemented the *Perceptron* function invented by MCCULLOCH and PITTS, an object that closely resembles the neural network structures still in use today. The perceptron is a function $\text{Perceptron}_{\boldsymbol{w},b} : \mathbb{R}^n \mapsto 0, 1$ defined as follows:

$$\text{Perceptron}_{\boldsymbol{w},b}(\boldsymbol{x}) = \begin{cases} 1 & \text{if } \boldsymbol{w} \cdot \boldsymbol{x} + b > 0, \\ 0 & \text{otherwise} \end{cases}$$

It only has binary output, on which it decides by performing a dot product between the weights vector $\boldsymbol{w} \in \mathbb{R}^n$ and the input, before adding a bias $b \in \mathbb{R}$ to it. When given a binary target dataset $\{\boldsymbol{x_i}, t_i\}$, the goal of the training process is to determine the weights $\boldsymbol{w}$ and bias b such that $\text{Perceptron}_{\boldsymbol{w},b}(\boldsymbol{x_i}) = t_i$ for as many samples as possible.

MCCULLOCH and PITTS further employed multiple consecutively connected perceptrons to form a larger 'network', each one referred to as a layer. Neural networks used today are remarkably similar in their structure (cf. figure 2.4). A neural network usually consists of multiple layers of potentially different types, commonly used ones include *Dense ('Fully Connected') Layers* (essentially, matrix multiplication + bias), *Convolutional Layers* (given a kernel, they perform a discrete multivariate convolution over the dataset) and mixtures of non-linear, differentiable, activation functions, max-pooling, etc. in between. Each Dense Layer is usually followed by an activation function such as

$$\text{relu}(\boldsymbol{x}) := \max(\boldsymbol{x}, 0)\,,$$

$$\text{softmax}(\boldsymbol{x}) := \frac{e^{\boldsymbol{x}}}{\sum_{i=1}^{n} e^{x_i}}\,,$$

$\tanh(\boldsymbol{x})$ or $\text{sigmoid}(\boldsymbol{x})$. They usually play the role of keeping the output bounded and/or sorting for 'activated' values (Bishop and Nasrabadi 2007).

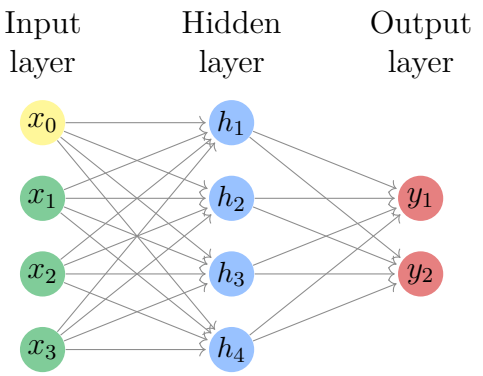

Figure 2.4: A simple neural network resembling the structure we use in our demonstrator, the input (a 784 entry vector) is forwarded to the second layer using $\boldsymbol{h} = \text{relu\_taylor}(M_1\boldsymbol{x} + \boldsymbol{b_1})$, resulting in a vector of 128 entries, and finally forwarded to the output layer with $\boldsymbol{y} = \text{softmax}(M_2\boldsymbol{h} + \boldsymbol{b_2})$. Each of the 10 outputs in $\boldsymbol{y}$ corresponds to a 'probability' associated with each digit from 0 to 9.

The training process is more complicated in the case of a layered network, especially with non-linear activation functions in between. Yet, the basic principle behind the training process stays the same: Evaluating the loss function L (depending on all weights, biases, convolutional kernels and other parameters in the network) and finding the direction in parameter space in

which the loss shrinks, formalised by the layer-wise gradient (for which we require the activation functions to be differentiable). The *Backpropagation Algorithm*, an interative process similar to GD, does exactly that: Evaluating the gradient of the loss function on the last layer and inversely forwarding the changes to the layer before it, and so on. From there, inferences on the weights, biases and other parameters can be made in order to update them for the next iteration and start over again, repeating the process, working ourselves towards the minimal loss possible (Bishop and Nasrabadi 2007).

As a final note to better understand the implications and possibilities of a large neural network, consider the following universal approximation theorem:

2.3.1 Theorem: Universal Approximation

If the neural network has at least one hidden layer, proper nonlinear activation functions and enough data and hidden units, it can approximate any continuous function $y(x, w) : \mathbb{R}^n \mapsto \mathbb{R}$ arbitrarily well on a compact domain (Hornik, Stinchcombe and White 1989).

In the case of our demonstrator, the network consists of two fully connected layers with a Taylor-approximated relu activation function in between. For more details on the implemented neural networks' structure, code and performance, refer to chapter 4 and chapter 5.

An alternative approach to modelling higher dimensional data would be *Gaussian Processes*, a Machine Learning technique with a focus on different applications than neural networks', but just as powerful (Mackay 2004, Chapter 45). The mathematical structure behind the model is a multivariate Gaussian distribution

$$p : \mathbb{R}^n \mapsto \mathbb{R},\ p(\boldsymbol{x}) = \frac{1}{\sqrt{(2\pi)^n |\Sigma|}} e^{-\frac{1}{2}(\boldsymbol{x}-\boldsymbol{\mu})^T \Sigma^{-1} (\boldsymbol{x}-\boldsymbol{\mu})},$$

in many cases allowing for explicit analytical expressions and calculations as compared to multi-layered neural networks.

2.4 Post-Quantum Security

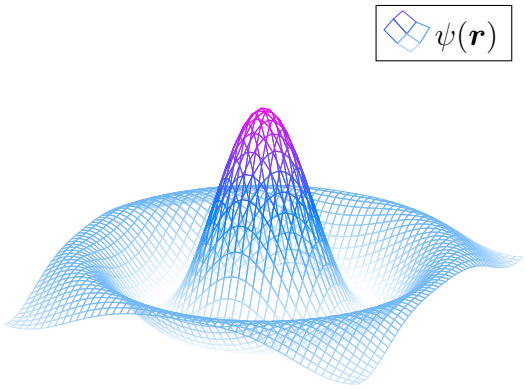

Figure 2.5: Illustration of a wave function ψ as commonly used in quantum mechanics. Its absolute value $|\psi(\boldsymbol{r}, t)|^2 = (\psi^* \psi)(\boldsymbol{r}, t)$ is a measure of the probability that a particle is currently at position $\boldsymbol{r}$ at time t.

In quantum mechanics, we seek a mathematical description of quantum phenomena, commonly building upon SCHRÖDINGER's formalisms based on wave functions and the basic postulates of quantum mechanics.

The mathematical foundation of quantum mechanics is deeply rooted in linear algebra and functional analysis. An important concept is that of function spaces and, especially, Hilbert spaces. Function spaces are a widely useful concept, polynomial rings are a great example too (confer corollary 2.1.1). Wave functions $\psi : \mathbb{C}^3 \times \mathbb{R} \mapsto \mathbb{C}$ are usually chosen as elements of the $\mathcal{L}^2$-space, the space of square-integrable[1] functions:

$$\mathcal{L}^2 = \left\{ \psi : \mathbb{C}^3 \times \mathbb{R} \mapsto \mathbb{C} \,\middle|\, ||\psi|| < \infty \right\} \quad \text{with } ||\psi|| = \int_{-\infty}^{\infty} \psi^*(\boldsymbol{x}) \psi(\boldsymbol{x}) \, d^3x$$

with $||\psi||$ referred to as the l_2-norm of the function ψ. By far not all functions are square integrable though, especially polynomials do not decrease in their absolute value towards $-\infty$ and ∞ leading to $||\psi|| \to \infty$, they are clearly not square integrable. An example that does work would be a normal distribution, or any function of the SCHWARTZ space.

The traditional Copenhagen interpretation relates a wave function to the probability that a particle is at the current position $\boldsymbol{r}$ at time t at the given time. Namely, this probability is given by $|\psi(\boldsymbol{r}, t)|^2$, see figure 2.5 for an exemplary illustration. The square-integrability requirement is imposed on the wave function ψ in order to make it normalizable, i.e. ensure that the total probability of presence is finite (or exactly 1) when integrated over all possible states the system might be in.

When describing a quantum particle or system, physicists usually work with mathematical objects in three different spaces:

- Position space inhibited by the wave function $\psi(\boldsymbol{r}, t) = \langle r | s_1, s_2, ..., s_n \rangle \in \mathcal{L}^2$ (a function space),

[1] Mathematicians usually formalise these using LEBESGUE-integrals instead of the commonly used RIEMANN formulation of an integral. LEBESGUE integration allows for a much broader class of integrable functions and is usually the preferred method in this context.

- Momentum space given by the Fourier-transformed wave function $\overline{\psi}(\boldsymbol{p}, t) = \langle p|s_1, s_2, ..., s_n\rangle \in \mathcal{L}^2$ (also a function space) and
- State space, encompassing all possible basis states in which a system might currently be, a description that is usually highly specific to the problem we aim to solve with it. In the discrete, finite-dimensional case, represented by $|s_1, s_2, ..., s_n\rangle \in \mathbb{S}$.

The electrons orbiting an atomic nucleus for instance, can be uniquely described by four quantum numbers (and corresponding Hermitian operators) forming a discrete state space: n, l, m_l and m_s with wave function $\langle r|n, l, m_l, m_s\rangle$ and momentum function $\langle p|n, l, m_l, m_s\rangle$.

Consider the following system of two base states $|0\rangle$ and $|1\rangle$, together forming an orthonormal basis. Due to *Quantum Superposition*, the measured system can be in any linear combination of the two,

$$|Q\rangle = \alpha\,|0\rangle + \beta\,|1\rangle\,,\ \alpha, \beta \in \mathbb{C}\,,$$

while enforcing that the scalar product of $\langle Q|$ with $|Q\rangle$ is normalized to 1 by the second axiom of probability theory, i.e.

$$\langle Q|Q\rangle = \Big(\alpha^*\,\langle 0| + \beta^*\,\langle 1|\Big)\Big(\alpha\,|0\rangle + \beta\,|1\rangle\Big) = |\alpha|^2 + |\beta|^2 \stackrel{!}{=} 1\,.$$

Here we use that $\{|0\rangle\,, |1\rangle\}$ comprise an orthonormal basis and therefore $\langle 0|1\rangle = 0$, $\langle 1|0\rangle = 0$, $\langle 0|0\rangle = 1$ and $\langle 1|1\rangle = 1$. This seemingly simple system is referred to as a *Qubit*, the basic unit of quantum information theory, uniquely represented by α and β.

Said to be 'at the heart of the disparity between classical and quantum physics', *Quantum Entanglement*, which Einstein once referred to as "spooky action at a distance", breaks the physical principle of locality but is yet a fundamental part of most quantum theories (Bell, Horne and Zeilinger 1989). This phenomenon describes the connection between two or more quantum particles related to each other through the mutual dependence of their quantum states $|s_1, s_2, ..., s_n\rangle$. Phrased differently, their states cannot be described independently of the rest of the particle group. For instance, two antisymmetrically entangled fermions never expose the same spin when measured simultaneously, even when they are far apart from each other - this has also been shown experimentally (Yin et al. 2013).

Quantum computers exploit the physical properties of quantum systems such as superposition and entanglement in order to speed up computations. They facilitate up to exponential speedups when algorithms are available, compared to problems on traditional computers. In conventional complexity theory, problems are filed into different complexity classes when analyzing their runtime and memory usage. There exist

1. NL (Nondeterministic Logarithmic space)
2. P (Polynomial time)
3. NP (Nondeterministic Polynomial time)
4. PSPACE (Polynomial space)
5. EXPTIME (Exponential time)
6. EXPSPACE (Exponential space)

computational complexity classes, sorted by the amount of problems contained in them (NL $\subseteq$ P $\subseteq$ NP $\subseteq$ PSPACE $\subseteq$ EXPTIME $\subseteq$ EXPSPACE). A particularly interesting open problem is whether P = NP, one of the millennium prize problems. The NP class of problems is particularly useful in cryptography, it is especially important for the hardness assumptions of cryptographic schemes, problems should be at least as hard as the hardest problems in NP.

2.4.1 Definition: NP-Hardness

A problem is referred to as *NP-hard* iff it is at least as hard as the hardest problems in the complexity class NP (nondeterministic polynomial time). Formally written,

$$\mathrm{NP} := \bigcup_{k \in \mathbb{N}} \mathrm{NTIME}(n^k)$$

the union of all decision problems with runtime bounded by $\mathcal{O}(n^k)$.

One of the first major algorithms in this context is Shor's algorithm, discovered before the first working quantum computer was built.

2.4.1 Shor's Algorithm

In the RSA scheme, but also other cryptographic schemes such as the Diffie-Hellman key exchange, the whole scheme's security is based on the hardness assumption of the integer factorisation problem. As of today, the cryptographic community still lacks a proof that the factorisation problem is in NP, yet it is widely believed to be. What we do know however, is that RSA encryptions can be broken and signatures forged, as soon as a sufficiently powerful quantum computer (with enough Qubits of memory) is built, in part explaining the global interest of governments and security organisations in the topic.

The algorithm enabling this was invented by Peter Shor in 1994 and will be outlined here shortly as it is a core element to security considerations of modern cryptosystems. The core structure of the algorithm is

1. randomly selecting a guess $g \in \mathbb{N}$ that we hope shares a factor with a large $N = p \cdot q$ $(p, q, N \in \mathbb{N})$,
2. improving that guess by a quantum subroutine and
3. applying Euclid's algorithm to find p and q the factors of N.

As soon as we found a guess g that satisfies $\gcd(N, g) \neq 1$, the algorithm finishes and we are done (Shor 1997).

The core factorisation idea is the following, not specific to quantum computation: We know that for a pair $g, N \in \mathbb{N}$, we can always find some $r \in \mathbb{N}$ such that

$$g^r = mN + 1,\ m \in \mathbb{N}\,,$$

we are looking for a g^r that is exactly one more than a multiple of N. Rearranging,

$$g^r - 1 = mN \iff (g^{\frac{r}{2}} + 1)(g^{\frac{r}{2}} - 1) = mN$$

we have found two factors $g^{\frac{r}{2}} + 1$ and $g^{\frac{r}{2}} - 1$ (for even r) that share a common factor with N and apply Euclid's algorithm to get p and q. These two factors $g^{\frac{r}{2}} + 1$, $g^{\frac{r}{2}} - 1$ might themselves be multiples of N, or r might be odd, rendering the guess useless and we need to start over with a new $g \in \mathbb{N}$. According to Shor 1997, we find 'good' factors roughly 35.7 % of the time with just one guess, with only ten tries we arrive at a success rate > 99 %. The plain guessing process can be done by any common computer, but is even more inefficient for large N (and resulting large r) than just factoring N using a general number field sieve (the state-of-the-art method of plain factorisation).

This is where the quantum component comes in, efficiently *improving* the guess g, therefore finding r. Using a quantum superposition, a quantum computer can calculate the output of a function for multiple superpositioned inputs *simultaneously*, which is what makes them so incredibly fast in some applications. When measuring the output state, the key idea of a quantum computation is to arrange the inputs in such a way that only useful output remains, while the other terms cancel each other out by destructive interference.

Thereby, we instruct the quantum computer to raise our guess g by all possible powers $\in \mathbb{N}$ up to some boundary in order to obtain

$$|1, g^1\rangle + |2, g^2\rangle + |3, g^3\rangle \, , ...$$

which we then take modulo N, resulting in a superposition of remainders

$$|1, [g^1]_N\rangle + |2, [g^2]_N\rangle + |3, [g^3]_N\rangle + ... \, .$$

Here is where Shor's key idea came in: The remainders in the above superposition expose repetitions at a period of exactly r (which, by our definition fulfills $g^r \equiv 1 \mod N$) because for any $a \in \mathbb{Z}$,

$$g^x \equiv g^{x+r} \equiv g^{x+2r} \equiv ... \equiv g^{x+ar} \mod N$$

the remainders are periodic with frequency $\frac{1}{r}$. The above can be quickly derived from $g^r = mN+1$, therefore

$$g^{x+r} = g^x g^r = (\tilde{m}N + [g^x]_N)(mN + 1) = (m\tilde{m}N + [g^x]_N m + \tilde{m})N + [g^x]_N$$

is indeed congruent to $g^x \mod N$.

And therefore, we can use a Quantum Fourier Transform (QFT), discovered by Don Coppersmith in 1994, on the superposition of remainders of powers of g to find the period r which is exactly what we were looking for. From the output of

$$\mathrm{QFT}\Big(|1, [g^1]_N\rangle + |2, [g^2]_N\rangle + |3, [g^3]_N\rangle + ...\Big)$$

we obtain the dominant frequency $\frac{1}{r}$ yielding us our desired improved guess (Shor 1997). Which again, can be evaluated extremely quickly on the given superpositioned inputs using a quantum computer, at least in theory. From here, we obtain $g^{\frac{r}{2}} + 1$ and $g^{\frac{r}{2}} - 1$ in order to finally find the factors p and q of N using Euclid's algorithm on $g^{\frac{r}{2}} \pm 1$ and N.

For large numbers N however, today's quantum computers' performance is still far off from factoring N into $p \cdot q$ effectively, for relatively small N however, it is already possible.

2.4.2 Outlook

Another important advancement in quantum computing related to cryptography is Grover's algorithm which provides an asymptotic quadratic speedup for performing function inversion (Grover 1996). It could be used to perform certain key recovery, collision or pre-image attacks on cryptographic schemes, essentially halving the bit security of many schemes (128 bit security would be reduced down to 64 bits), suggesting to double the involved key size bits in many encryption schemes in order to be safe against potential future quantum attacks.

Lattice-based cryptosystems are still safe against quantum computation, i.e. quantum computers have a negligible advantage compared to traditional computers when attempting to break lattice-based encryptions, performing key-recovery attacks, etc. Two of these schemes will be presented in the next chapter, in section 3.3 and section 3.4.

Chapter 3

Homomorphic Encryption

HE makes it possible to operate on data without knowing it. One can distinguish three flavors of it, Partial-, Somewhat-, Levelled- and Fully Homomorphic Encryption (FHE).

For FHE, there exist a few schemes in use today with existing implementations.

- BFV scheme for integer arithmetic (Fan and Vercauteren 2012; Brakerski 2012).
- BGV scheme for integer arithmetic (Brakerski, Gentry and Vaikuntanathan 2012).
- CKKS scheme for (complex) floating point arithmetic (Cheon et al. 2017).
- Fastest Homomorphic Encryption in the West (FHEW) scheme for Boolean circuit evaluation (Ducas and Micciancio 2015).
- Torus Fully Homomorphic Encryption (TFHE) scheme for Boolean circuit evaluation (Chillotti et al. 2019).

We will first introduce the BFV scheme (integer arithmetic) as it represents a fundamental building block behind CKKS. Due to the inherent applications, this thesis will focus on the CKKS scheme to perform homomorphic operations on (complex-valued) floating point numbers and vectors.

To alleviate upcoming notation, for two tuples $(\cdot, \cdot)$ defined over the same ring, denote their element-wise addition as $(\cdot, \cdot) + (\cdot, \cdot)$, element-wise multiplication by a scalar u as $u \cdot (\cdot, \cdot)$ and element-wise rounding as $\lfloor (\cdot, \cdot) \rceil$.

3.1 Homomorphic Encryption using RSA

In order to illustrate the basic idea behind HE, without distancing ourselves too far from the original goal of introducing basic HE operations used in practice, this short section aims to motivate the definition of ring homomorphisms (cf. definition 3.1.1) behind a cryptographic background.

With unpadded RSA (R. L. Rivest, Shamir and L. M. Adleman 1983), some arithmetic can be performed on the ciphertext - looking at the encrypted ciphertext $\mathcal{E} : \mathbb{Z}/q\mathbb{Z} \mapsto \mathbb{Z}/q\mathbb{Z}$, $\mathcal{E}(m) := m^r$

mod q ($r, q \in \mathbb{N}$) of the message $m_1, m_2 \in \mathbb{Z}/q\mathbb{Z}$ respectively, the following holds:

$$\begin{aligned}\mathcal{E}(m_1) \cdot \mathcal{E}(m_2) &\equiv (m_1)^r (m_2)^r \mod q \\ &\equiv (m_1 m_2)^r \mod q \\ &\equiv \mathcal{E}(m_1 \cdot m_2) \mod q\end{aligned}$$

RSA encryption (even supporting an unbounded number of modular multiplications) therefore fulfills the properties of a multiplicative ring homomorphism, which in general terms is defined as follows:

3.1.1 Definition: Ring Homomorphism

Given two rings $(R, +, \cdot)$ and $(S, \oplus, \otimes)$, we call a mapping $\varphi : R \to S$ a ring homomorphism when it satisfies the following conditions:

$$\forall a, b \in R : \varphi(a + b) = \varphi(a) \oplus \varphi(b) \land \varphi(a \cdot b) = \varphi(a) \otimes \varphi(b)$$

As we can see, the term Homomorphic Encryption originates from the ability to perform computations on encrypted data while ensuring the same results are obtained when the same operations are applied to the original data.

3.2 Gentry's FHE-Scheme and BGV

Homomorphic encryption was envisioned by R. Rivest, L. Adleman and Dertouzos as early as the 70s but remained a phantasm for almost three decades and was since referred to as the 'holy grail' of cryptography. The first fully homomorphic encryption scheme was introduced in Craig Gentry's PhD thesis, based on lattice problems (Gentry 2009). In earlier schemes, each HE operation increases noise, making it partially homomorphic instead of fully homomorphic encryption. Gentry devised a technique called *bootstrapping* that evaluates the *decryption* circuit homomorphically and thereby resets the noise introduced by previous operations, enabling true fully homomorphic encryption (FHE). Followup schemes improved his blueprint, Gentry's work is clearly a landmark achievement (Micciancio 2010).

Brakerski, Gentry and Vaikuntanathan 2012 developed a generalisation of RLWE that enables interpolation between LWE and RLWE, allowing for many improvements on earlier schemes, though mainly relying on Gentry 2009. The resulting scheme, referred to as BGV, allows for integer arithmetic (addition and multiplication on $\mathbb{Z}/q\mathbb{Z}$). It also employs a modulus reduction technique, greatly extending the homomorphic capacity to a broader class of homomorphic circuits. *Microsoft SEAL 4.0* 2022 implements the scheme, enabled using `seal::scheme_type::bgv`.

3.3 The BFV Scheme

This scheme was developed in two separate publications, whose authors initials it is named after, Brakerski 2012 and Fan and Vercauteren 2012. BFV is based on BGV and they are really similar in their core ideas, one can even convert a BFV ciphertext to an equivalent BGV ciphertext (A. Kim, Polyakov and Zucca 2021). In this section, we will focus on a slightly altered implementation introduced in Lepoint and Naehrig 2014.

3.3.1 Scheme Definition

The BFV scheme is a tuple of algorithms, introduced in definition 3.3.1. To summarise the occuring parameters and variables, a brief overview of all used symbols is provided in table 3.1.

3.3.1 Definition: The BFV-Scheme

Let $R = \mathbb{Z}[X]/\Phi_d(X)$ be a polynomial ring with $\Phi_d(X)$ the d^{th} cyclotomic polynomial ($\rightarrow d \in \mathbb{N}$) for ciphertexts $c \in R \times R$. Introduce R/qR the associated quotient ring of the q^{th} coset of R with the modulus $q \in \mathbb{N}$. Further let $t \in \mathbb{N}$ denote the message modulus with $1 < t < q$ for plain messages $m \in R/tR$ and define $\delta := \lfloor \frac{q}{t} \rfloor$, $\delta^{-1} = \frac{t}{q}$.
Introduce three bounded discrete probability distributions χ_{key}, χ_{enc} and χ_{error} over R/qR, one which is only used once for key generation, another used for BFV.Encrypt and another (usually Gaussian-like) error distribution for manually inserted error terms (confer the LWE-problem). For BFV, usually $\chi_{key} = \chi_{enc}$.
For a polynomial $a \in R/qR$, consider the decomposition $a = \sum_{i=0}^{l-1} a_i w^i$ into base $w \in \mathbb{N}$ obtained by $\text{WordDecomp} : R \mapsto R^l$, $\text{WordDecomp}(a) = ([a_i]_w)_{i=0}^{l-1}$.
Further let $\text{PowersOf} : R \mapsto R^l$ be defined as $\text{PowersOf}(a) = ([aw^i]_q)_{i=0}^{l-1}$.
Let the parameters $\mathbb{P} = (d, q, t, \chi_{key}, \chi_{error}, w)$ and $l = \lfloor \log_w(q) \rfloor + 1$.

BFV.

$\text{ParamGen}(\lambda)$	Choose parameters as defined above, given the security parameter λ, such that $1 < t < q$, $w \geq 2$, initialize distributions χ_{key}, χ_{enc} and χ_{error} $\quad \rightarrow \mathbb{P}$
$\text{KeyGen}(\mathbb{P})$	Generate the secret key $s \leftarrow \chi_{key}$, sample $\boldsymbol{\mu} \in (R/qR)^l$ from χ_{error} and choose some $\boldsymbol{a} \in (R/qR)^l$ uniformly at random, compute the relinearisation key $\boldsymbol{\gamma} = (\text{PowersOf}(s^2) - (\boldsymbol{\mu} + \boldsymbol{a} \cdot s), \boldsymbol{a})$ and finally output the public key for uniformly random $a \in (R/qR)$ and $\mu \leftarrow \chi_{error}$ with $b = -(a \cdot s + \mu)$ as $\boldsymbol{p} = (b, a)$. $\quad \rightarrow \boldsymbol{p}, s, \boldsymbol{\gamma}$
$\text{Encrypt}(\boldsymbol{p}, m)$	Let $(b, a) = \boldsymbol{p}$, $u \leftarrow \chi_{enc}$, $\mu_1, \mu_2 \leftarrow \chi_{error}$, then the ciphertext is $\boldsymbol{c} = u \cdot \boldsymbol{p} + (\delta m + \mu_1, \mu_2) = (\delta m + bu + \mu_1, au + \mu_2) \quad \rightarrow \boldsymbol{c}$
$\text{Decrypt}(s, \boldsymbol{c})$	Decrypt $\boldsymbol{c} = (c_0, c_1)$ as $m = \lfloor \delta^{-1}[c_0 + c_1 s]_t \rceil \in R/tR \quad \rightarrow m$
$\text{Add}(\boldsymbol{c}_1, \boldsymbol{c}_2)$	Let $(c_0^1, c_1^1) = \boldsymbol{c}_1$ and $(c_0^2, c_1^2) = \boldsymbol{c}_2$ then $\boldsymbol{c}_3 = (c_0^1 + c_0^2, c_1^1 + c_1^2) = \boldsymbol{c}_1 + \boldsymbol{c}_2 \quad \rightarrow \boldsymbol{c}_3$
$\text{Mult}(\boldsymbol{c}_1, \boldsymbol{c}_2)$	Output $\overline{\boldsymbol{c}} = (\lfloor \delta^{-1} c_0^1 c_0^2 \rceil, \lfloor \delta^{-1}(c_0^1 c_1^2 + c_1^1 c_0^2) \rceil, \lfloor \delta^{-1} c_1^1 c_1^2 \rceil) \quad \rightarrow \overline{\boldsymbol{c}}$
$\text{ReLin}(\overline{\boldsymbol{c}}, \boldsymbol{\gamma})$	Using the relin key $\boldsymbol{\gamma} = (\boldsymbol{b}, \boldsymbol{a})$, relinearize from $\overline{\boldsymbol{c}} = (c_0, c_1, c_2)$ as $\boldsymbol{c} = (c_0 + \text{WordDecomp}(c_2) \cdot \boldsymbol{b}, c_1 + \text{WordDecomp}(c_2) \cdot \boldsymbol{a}) \quad \rightarrow \boldsymbol{c}$

(Fan and Vercauteren 2012; Brakerski 2012)

Table 3.1: Summary of the parameters and symbols in BFV.

Symbol	Space	Explanation
λ	$\in \mathbb{R}$	Security parameter
d	$\in \mathbb{N}$	Index of the cyclotomic polynomial used in R
q	$\in \mathbb{N}$	Modulus of the ciphertext space R/qR
t	$\in \mathbb{N}$	Modulus of the plaintext message space R/tR
δ	$\in \mathbb{N}$	Ratio between ciphertext and plaintext modulus
δ^{-1}	$\in \mathbb{R}$	Inversion coefficient of the effect of δ
w	$\in \mathbb{N}$	Word size used as basis, e.g. $w = 2$ for bits
l	$\in \mathbb{N}$	Number of words of size w required to encode q
s	$\in R$	Secret Key
$\boldsymbol{p}$	$\in (R/qR)^2$	Public Key (b, a)
$\boldsymbol{\gamma}$	$\in [(R/qR)^l]^2$	Relinearisation Key
m	$\in R/tR$	Plaintext Message
$\boldsymbol{c}$	$\in (R/qR)^2$	Ciphertext
$\bar{\boldsymbol{c}}$	$\in (R/qR)^3$	Slightly larger ciphertext resulting from multiplication

Parameters in $\mathbb{P}$ described above need to be carefully chosen in order to provide for a certain security level λ [1]. Also note that q or t do not need to be prime and could be chosen e.g. as powers of 2. Encryption requires the public key, decryption the private key as usual in public-key encryption schemes. The public key depends on the secret key and is chosen in such a way that the corresponding term cancels out when decrypting, as can be seen in section 3.3.2.

Homomorphic Addition, by design, works by simple addition of the corresponding ciphertexts. Multiplication is based on a similar procedure, but tries to prevent an explosion of the scale by dividing through δ in all three terms. Otherwise, the original input would be proportional to δ^2 after multiplication, instead of δ as expected when decrypting. The BFV.ReLin operation then takes care of merging the three-term tuple back into a ciphertext made of two polynomials using the relinearisation key $\boldsymbol{\gamma}$.

The diagram in figure 3.1 shows how a typical encryption process works and which ring each object is part of, also compare table 3.1.

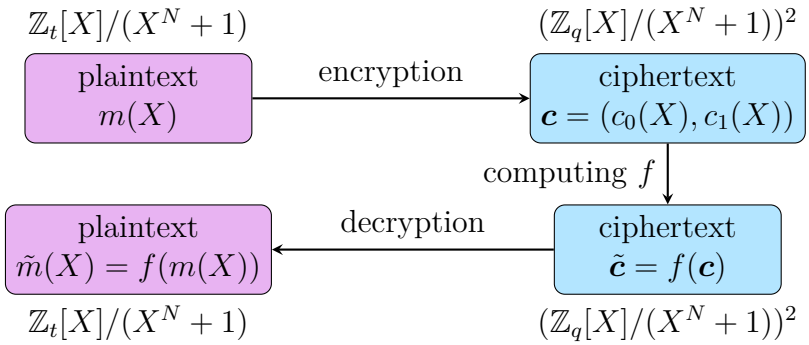

Figure 3.1: Schematic overview of the BFV scheme, adapted from Huynh 2020. A plaintext polynomial $m(X)$ is encrypted to the ciphertext $\boldsymbol{c} = \text{BFV.Encrypt}(\boldsymbol{p}, m)$ using the public key $\boldsymbol{p}$, operated on using a combination of BFV.{Add, Mult, ReLin} ciphertext operations and finally decrypted to a new $\tilde{m} = \text{BFV.Decrypt}(s, \tilde{\boldsymbol{c}})$ using the secret key s.

[1] for example, using https://github.com/malb/lattice-estimator

3.3.2 Verification of the Additive Homomorphism

3.3.1 Theorem: BFV encryption is homomorphic with respect to addition

BFV.Encrypt should encrypt in such a way that the addition algebra can be retained even in the transformed space, showing that we can indeed refer to it as homomorphic encryption.

Proof. Starting out with two messages $m, m' \in R/tR$, two polynomials of degree $N-1$ with N coefficients modulo t, we check whether addition of two ciphertexts $\boldsymbol{c} = \text{BFV.Encrypt}(\boldsymbol{p}, m)$ and $\boldsymbol{c}' = \text{BFV.Encrypt}(\boldsymbol{p}, m')$ indeed decrypts as $m + m'$.

The client first creates a secret key s and public key $\boldsymbol{p} = (b, a)$ with $b = -(as + \tilde{\mu})$ using $\text{BFV.ParamGen}(\lambda)$ and $\text{BFV.KeyGen}(\mathbb{P})$. Encrypting m and m' using the public key, we obtain

$$\boldsymbol{c} = (c_0, c_1) = \begin{pmatrix} \delta m + bu + \mu_1 \\ au + \mu_2 \end{pmatrix}^T \quad \text{and} \quad \boldsymbol{c}' = (c_0', c_1') = \begin{pmatrix} \delta m' + bu' + \mu_1' \\ au' + \mu_2' \end{pmatrix}^T .$$

Evaluating $\overline{\boldsymbol{c}} := \text{BFV.Add}(\boldsymbol{c}, \boldsymbol{c}') = \boldsymbol{c} + \boldsymbol{c}'$,

$$\overline{\boldsymbol{c}} = \begin{pmatrix} \delta(m+m') + b(u+u') + (\mu_1 + \mu_1') \\ a(u+u') + (\mu_2 + \mu_2') \end{pmatrix}^T = \begin{pmatrix} \delta\overline{m} + b\overline{u} + \overline{\mu_1} \\ a\overline{u} + \overline{\mu_2} \end{pmatrix}^T$$

we obtain a ciphertext that decrypts to the correct sum. Indeed,

$$\begin{aligned}
\text{BFV.Decrypt}(s, \overline{\boldsymbol{c}}) &= \lfloor \delta^{-1}[\overline{c_0} + \overline{c_1}s]_t \rceil \\
&= \left\lfloor \delta^{-1}[\delta\overline{m} + b\overline{u} + \overline{\mu_1} + (a\overline{u} + \overline{\mu_2})s]_t \right\rceil \\
&= \left\lfloor [(\delta^{-1}\delta)\overline{m} + \delta^{-1}b\overline{u} + \delta^{-1}\overline{\mu_1} + \delta^{-1}as\overline{u} + \delta^{-1}\overline{\mu_2}s]_t \right\rceil \\
&= \left\lfloor [\overline{m} - \delta^{-1}(as + \tilde{\mu})\overline{u} + \delta^{-1}\overline{\mu_1} + \delta^{-1}as\overline{u} + \delta^{-1}\overline{\mu_2}s]_t \right\rceil \\
&= \left\lfloor [\overline{m} - \cancel{\delta^{-1}as\overline{u}} - \delta^{-1}\tilde{\mu}\overline{u} + \delta^{-1}\overline{\mu_1} + \cancel{\delta^{-1}as\overline{u}} + \delta^{-1}\overline{\mu_2}s]_t \right\rceil \\
&= \left\lfloor [\overline{m} + \underbrace{\delta^{-1}(\overline{\mu_1} + \overline{\mu_2}s - \tilde{\mu}\overline{u})}_{:=\epsilon,\, ||\epsilon|| \ll 1}]_t \right\rceil \approx \left\lfloor [\overline{m}]_t \right\rceil = \lfloor \overline{m} \rceil \approx \overline{m}
\end{aligned}$$

we arrive at the desired result $\overline{m} = m + m'$ after rounding ($\lfloor \cdot \rceil$) the (real) polynomial to a close element in R/tR using one of several round-off algorithms (cf. Lyubashevsky, Peikert and Regev 2013). Of course, the influx of ϵ is only neglible if all parameters are carefully chosen as described in definition 3.3.1 and the error terms are sufficiently small.

$$t \ll q \implies \delta^{-1} = t/q \ll 1$$

should be given while also ensuring that the spread of the distributions χ_{key}, χ_{enc} and χ_{error} is not too large so that $\overline{\mu_{1,2}}, \overline{u}$ and $\tilde{\mu}$ do not lead to a large ϵ distorting our final result. □

As the public key $\boldsymbol{p} = (b, a)$ corresponds to a sample from the RLWE distribution (corollary 2.2.1), the implied security of the BFV scheme is given by the hardness assumption of LWE (theorem 2.2.1). An attacker trying to decrypt a ciphertext $\boldsymbol{c}$, given only the public key $\boldsymbol{p}$, would thereby need to solve the RLWE search problem (corollary 2.2.2) which is known to be hard (Lyubashevsky, Peikert and Regev 2010).

Microsoft SEAL 4.0 2022 implements the scheme, enabled using `seal::scheme_type::bfv`.

3.4 The CKKS Scheme

The CKKS scheme allows us to perform approximate arithmetic on floating point numbers. Essentially, the idea is to extend BFV which allows us to operate on polynomials $p \in R/qR$, by an embedding approach that allows us to encode a (complex) floating point number vector $\boldsymbol{z} \in \mathbb{R}^n\,(\mathbb{C}^n)$ as an integer polynomial, similar to what is used in BFV. A main contribution of CKKS is that we have a homomorphic rounding operation which allows to reduce the scaling factors after mulitplication. The remaining scheme is then extremely similar to BFV and even more to BGV which it is based on.

Introduce $d, R, R/qR$ as in definition 3.3.1 and further define $\mathcal{S} = \mathbb{R}[X]/\Phi_d(X) \subset R$ a similar polynomial ring to R, but over the reals instead of the integers. Let $N = \varphi(d)$ be the degree of the reducing cyclotomic polynomial of $\mathcal{S}$, confer definition 2.1.6. For convenience, we usually choose d a power of 2 and then, by theorem 2.1.1, $N = \varphi(d) = \frac{d}{2}$ which yields efficiently multipliable polynomials because the homomorphic multiplication operation can be performed using a Discrete Fourier Transform (DFT) and further optimized using the Fast Fourier Transform (FFT), which in its unmodified form only accepts power-of-2 vector sizes (Cheon et al. 2017).

3.4.1 Encoding and Decoding

In addition to encryption and decryption, the CKKS scheme also defines the CKKS.Encode and CKKS.Decode operations, extending possible plain inputs from polynomials $m \in R$ (as in BFV) to complex-valued vectors $\boldsymbol{z} \in \mathbb{C}^{N/2}$ [2]. When encoding a vector of $N/2$ elements into a polynomial, a main goal is of course to ensure that addition and multiplication then correspond to elementwise vector addition and multiplication. Furthermore, these vectors can be rotated (i.e. shifting the elements by an offset) using the *Galois automorphism*. We will not discuss it in detail here, nevertheless Galois rotations are heavily used in the implementation to facilitate effective matrix multiplications (confer section 4.4). In total, the encoding and decoding steps consist of three transformations, $\underline{\pi}$, $\underline{\rho}$ and $\underline{\sigma}$.

3.4.1 Definition: Canonical Embedding $\underline{\sigma}$

For a real-valued polynomial $p \in \mathcal{S}$, define the canonical embedding of $\mathcal{S}$ in $\mathbb{C}^N$ as a mapping $\underline{\sigma} : \mathcal{S} \mapsto \mathbb{C}^N$ with

$$\underline{\sigma}(p) := \left(p(e^{-2\pi i j/N})\right)_{j \in \mathbb{Z}_d^*}$$

with $\mathbb{Z}_d^* := \{x \in \mathbb{Z}/d\mathbb{Z} \,|\, \gcd(x, d) = 1\}$ the set of all integers smaller than d that do not share a factor > 1 with d. The image of $\underline{\sigma}$ given a set of inputs R shall be denoted as $\underline{\sigma}(R) \subseteq \mathbb{C}^N$. Let the inverse of $\underline{\sigma}$ be denoted by $\underline{\sigma}^{-1} : \mathbb{C}^N \mapsto \mathcal{S}$.

All elements of R are also elements of $\mathcal{S}$ since $\mathbb{Z} \subset \mathcal{S}$ which results in $\underline{\sigma}(R) \subset \underline{\sigma}(\mathcal{S})$, every plaintext polynomial $m \in R$ can be encoded into $\underline{\sigma}(R)$. Also note that evaluating a polynomial on the n^{th} roots of unity corresponds to performing a Fourier-Transform.

Define the commutative subring $(\mathbb{H}, +, \cdot)$ of $(\mathbb{C}^N, +, \cdot)$ on the set

$$\mathbb{H} := \{\boldsymbol{z} = (z_j)_{j \in \mathbb{Z}_d^*} \in \mathbb{C}^N : z_j = \overline{z_{-j}}\ \forall j \in \mathbb{Z}_d^*\} \subseteq \mathbb{C}^N$$

[2] Many implementations of BFV provide similar encoding and decoding procedures, extending the original BFV scheme (Fan and Vercauteren 2012) to facilitate encrypted vector arithmetic.

of all complex-valued vectors $\boldsymbol{z}$ where the first half equals the reversed complex-conjugated second half.

3.4.2 Definition: Natural Projection $\underline{\pi}$

Let T be a mulitplicative subgroup of $\mathbb{Z}_d^*$ with $\mathbb{Z}_d^*/T = \{\pm 1\} = \{1T, -1T\}$, then the natural projection $\underline{\pi} : \mathbb{H} \mapsto \mathbb{C}^{N/2}$ is defined as

$$\underline{\pi}\Big((z_j)_{j\in\mathbb{Z}_M^*}\Big) := (z_j)_{j\in T}$$

Let its inverse be denoted by $\underline{\pi}^{-1} : \mathbb{C}^{N/2} \mapsto \mathbb{H}$ and consequently defined as

$$\underline{\pi}^{-1}\Big((z_j)_{j\in T}\Big) := \Big(\nu(z_j)\Big)_{j\in\mathbb{Z}_M^*} \text{ with } \nu(z_j) = \begin{cases} z_j & \text{if } j \in T \\ \overline{z_j} & \text{otherwise} \end{cases}$$

The natural projection $\underline{\pi}$ simply halves a vector $\boldsymbol{z} \in \mathbb{H}$ to all elements where $j \in T$ to only contain its essential information (the first half), since the second half can easily be reconstructed by element-wise conjugation using ν. The exact structure of T is given by $\mathbb{Z}_d^*/T = \{\pm 1T\}$ with $+1T$ and $-1T$ denoting multiplicative left cosets of T, together forming the quotient group $(\mathbb{Z}_d^*/T, \cdot)$ over multiplication (denoted $\cdot$ instead of $+$ as in the quotient group definition in the previous chapter).

Further studying T. We first notice that by Lagrange's theorem on finite groups, the number of elements in T is exactly $N/2$ since

$$\frac{|\mathbb{Z}_d^*|}{|T|} = |\{\pm 1\}| \Leftrightarrow \frac{N}{|T|} = 2 \Leftrightarrow |T| = \frac{N}{2}$$

leading to $\underline{\pi}(\mathbb{H}) \subseteq \mathbb{C}^{N/2}$. Rephrased, we seek a $T \subseteq \mathbb{Z}_d^*$ with $1 \in T$ such that we can fully construct $\mathbb{Z}_d^*$ by the union of the cosets $1T$ and $-1T$, i.e. $\mathbb{Z}_d^* = (1T) \cup (-1T)$. Note that T is not unique, we can find multiple sets T for which the above holds, for instance by brute force computation:

```python
import itertools, math, numpy as np
d = 16; Zdstar = [z for z in range(d) if math.gcd(d, z) == 1]
possible_T = [T for T in itertools.combinations(Zdstar, len(Zdstar) // 2)
  if 1 in T and list(np.unique(list(T) + [(-1*t) % d for t in T])) == Zdstar]
```

Example. Let $d = 16$, then $\mathbb{Z}_d^* = \{1, 3, 5, 7, 9, 11, 13, 15\}$ and $N = |\mathbb{Z}_d^*| = 8$ and by Lagrange's theorem, $|T| = 4$. Since $(T, \cdot)$ forms a normal subgroup under multiplication, we must have that $1 \in T$ and we can identify all possible subgroups T satisfying $\mathbb{Z}_d^*/T = \{\pm 1T\}$ to be one of

$$\{1, 3, 5, 7\}, \{1, 3, 5, 9\}, \{1, 3, 7, 11\}, \{1, 3, 9, 11\},$$
$$\{1, 5, 7, 13\}, \{1, 5, 9, 13\}, \{1, 7, 11, 13\}, \{1, 9, 11, 13\}$$

using the above Python code. An example of an invalid subset T that does cover the whole original set $\mathbb{Z}_d^*$ would be $T = \{1, 7, 9, 15\}$.

For the purposes of CKKS, we simply choose a global T that is constant for our encoding and decoding procedure and a given d. The inverse natural projection $\underline{\pi}^{-1}$ then uniquely constructs a vector in $\mathbb{H}$ by filling in elements $\overline{z_j}$ for $j \notin T$ into $\boldsymbol{z}$. For simplicity, we commonly choose T as the 'first half' of $\mathbb{Z}_d^*$ when sorting in an ascending manner as it is always a valid choice [3].

3.4.3 Definition: Discretisation to an element of $\underline{\sigma}(R)$

Using one of several round-off algorithms (cf. Lyubashevsky, Peikert and Regev 2013), given an element of $\mathbb{H}$, define a rounding operation $\underline{\rho}^{-1} : \mathbb{H} \mapsto \underline{\sigma}(R)$ that maps an $\boldsymbol{h} \in \mathbb{H}$ to its closest element in $\underline{\sigma}(R) \subset \mathbb{H}$, also denoted as

$$\underline{\rho}^{-1}(\boldsymbol{h}) := \lfloor \boldsymbol{h} \rceil_{\underline{\sigma}(R)} .$$

Further let $\underline{\rho_\delta}^{-1}(\boldsymbol{h}) = \lfloor \delta \cdot \boldsymbol{h} \rceil_{\underline{\sigma}(R)}$ denote the same rounding operation but with prior scaling by a scalar factor δ. Note that $\underline{\rho}$ is given directly as the identity operation because all elements of its domain are already elements of its image. Similarly, $\underline{\rho_\delta}^{-1}(\boldsymbol{y}) = \delta^{-1} \cdot \boldsymbol{y}$.

Because it is not essential to understanding the encryption scheme, we will skip over concrete implementations of the rounding procedure $\underline{\rho}^{-1}$. For choosing a *close* element $\boldsymbol{g} \in \mathbb{H}$, we must first introduce a sense of proximity, in this case done by the l_∞-norm $||\boldsymbol{g} - \boldsymbol{h}||_\infty$ of the difference between $\boldsymbol{h} \in \mathbb{H}$ and $\boldsymbol{g}$.

All in all, $m = \text{CKKS.Encode}(\boldsymbol{z})$, $\boldsymbol{z} \in \mathbb{C}^{N/2}$ applies all inverse transformations $\underline{\pi}^{-1}$ (first), $\underline{\rho}^{-1}$ (second) and $\underline{\sigma}^{-1}$ (third) to an input vector $\boldsymbol{z}$ in order to finally arrive at a plaintext polynomial $m \in R/q_L R$ (equally stated as $m \in \mathbb{Z}_{q_L}/(X^N + 1)$ as long as N is a power of 2). Although $\underline{\sigma}$ is defined over $\mathcal{S}$ instead of $\mathcal{R}$, all elements of $\underline{\sigma}(R)$ can indeed be mapped back to an element in R using $\underline{\sigma}^{-1}$. Summarised,

$$\mathbb{C}^{N/2} \xrightarrow{\underline{\pi}^{-1}} \mathbb{H} \xrightarrow{\underline{\rho}^{-1}} \sigma(R) \xrightarrow{\underline{\sigma}^{-1}} R .$$

The decoding procedure $\boldsymbol{z} = \text{CKKS.Decode}(m)$, $m \in R$ does the opposite to reobtain the input vector $\boldsymbol{z} \in \mathbb{C}^{N/2}$.

It should also be noted that the encoding procedure represents an isometric ring isomorphism (a linear bijection that preserves distance) between its domain and image, as does the decoding procedure. This reflects in the observation that the plaintext sizes and errors are preserved under the transformations (Cheon et al. 2017).

[3] This can be seen from the coset $-1T$ which exactly equals the 'missing' half in $\mathbb{Z}_d^*$ when the first half is covered by $1T = T = \{1, 3, 5, ..., N-1\}$ since $-1T = \{-1, -3, -5, ..., -(N-1)\} \equiv \{d-1, d-3, d-5, ..., d-N+1\} \pmod d$ when d a power of 2. Then, $(1T) \cup (-1T) = \{1, 3, 5, ..., N-1\} \cup \{d-1, d-3, d-5, ..., d-N+1\} = \{1, 3, 5, ..., N-1, N+1, ..., d-5, d-3, d-1\} = \mathbb{Z}_d^*$.

3.4.2 Scheme Definition

The BFV scheme is a tuple of algorithms, introduced in definition 3.3.1. To summarise the occuring parameters and variables, a brief overview of all used symbols is provided in table 3.2.

3.4.4 Definition: The CKKS Scheme

Define $R, R/q_L R$ as in definition 3.3.1. Introduce three bounded discrete probability distributions χ_{key}, χ_{enc} and χ_{error} over $R/q_L R$.

CKKS.

ParamGen(λ)	Choose parameters as defined above, given the security parameter λ and space modulus q_L, choose $d \in \mathbb{N}$ a power of 2, $P, h \in \mathbb{Z}$, $\sigma \in \mathbb{R}$ and initialize distributions χ_{key}, χ_{enc} and χ_{error}. $\rightarrow \mathbb{P}$
KeyGen($\mathbb{P}$)	Sample the secret key $s \leftarrow \chi_{key}$, $a \in R_{q_L}$ uniformly at random, $\mu \leftarrow \chi_{error}$ and obtain the public key $\boldsymbol{p} = (b, a)$ with $b = -a \cdot s + \mu$. Sample $a' \in R_{P \cdot q_L}$ uniformly at random, $\mu' \leftarrow \chi_{error}$ and obtain the evaluation key $\boldsymbol{\gamma} = (b', a')$ with $b' = -a' \cdot s + \mu' + Ps^2$. $\rightarrow \boldsymbol{p}, s, \boldsymbol{\gamma}$
Encode($\boldsymbol{z}$)	For a given input vector $\boldsymbol{z}$, output $m = (\underline{\sigma}^{-1} \circ \underline{\rho_\delta}^{-1} \circ \underline{\pi}^{-1})(\boldsymbol{z}) = \underline{\sigma}^{-1}(\lfloor \delta \cdot \underline{\pi}^{-1}(\boldsymbol{z}) \rceil_{\sigma(R)})$ $\rightarrow m$
Decode(m)	Decode plaintext m as $\boldsymbol{z} = (\underline{\pi} \circ \underline{\rho_\delta} \circ \underline{\sigma})(m) = (\underline{\pi} \circ \underline{\sigma})(\delta^{-1} m)$ $\rightarrow \boldsymbol{z}$
Encrypt($\boldsymbol{p}, m$)	Let $(b, a) = \boldsymbol{p}$, $u \leftarrow \chi_{enc}$, $\mu_1, \mu_2 \leftarrow \chi_{error}$, then the ciphertext is $\boldsymbol{c} = u \cdot \boldsymbol{p} + (m + \mu_1, \mu_2) = (m + bu + \mu_1, au + \mu_2)$ $\rightarrow \boldsymbol{c}$
Decrypt($s, \boldsymbol{c}$)	Decrypt the ciphertext $\boldsymbol{c} = (c_0, c_1)$ as $m = [c_0 + c_1 s]_{q_L}$ $\rightarrow m$
Add($\boldsymbol{c}_1, \boldsymbol{c}_2$)	Output $\boldsymbol{c}_3 = \boldsymbol{c}_1 + \boldsymbol{c}_2$ $\rightarrow \boldsymbol{c}_3$
Mult($\boldsymbol{c}_1, \boldsymbol{c}_2$)	Output $\overline{\boldsymbol{c}} = (c_0^1 c_0^2, c_0^1 c_1^2 + c_1^1 c_0^2, c_1^1 c_1^2)$ $\rightarrow \overline{\boldsymbol{c}}$
ReLin($\overline{\boldsymbol{c}}, \boldsymbol{\gamma}$)	Using the evaluation key $\boldsymbol{\gamma}$, relinearize from $\overline{\boldsymbol{c}} = (c_0, c_1, c_2)$ to $\boldsymbol{c} = (c_0, c_1) + \lfloor P^{-1} c_2 \boldsymbol{\gamma} \rceil$ $\rightarrow \boldsymbol{c}$
ReScale($\boldsymbol{c}$)	In order to rescale a ciphertext from level l_{old} to l_{new}, multiply by a factor $\frac{q_{l_{new}}}{q_{l_{old}}} \in \mathbb{Q}$ and round to the nearest element of $(R/q_{l_{new}} R) \times (R/q_{l_{new}} R)$: $\boldsymbol{c}_{new} = \left\lfloor \frac{q_{l_{new}}}{q_{l_{old}}} \boldsymbol{c} \right\rceil$ $\rightarrow \boldsymbol{c_{new}}$

(Cheon et al. 2017)

For more details on the probability distributions, refer to the original CKKS paper (Cheon et al. 2017), with the following naming relations: $\chi_{key} = \mathcal{HWT}(h)$ over $\{0, \pm 1\}^N$, $\chi_{error} = \mathcal{DG}(\sigma^2)$ over $\mathbb{Z}^N$ and $\chi_{enc} = \mathcal{ZO}(0.5)$ another distribution over $\{0, \pm 1\}^N$.

Encryption, decryption, addition and multiplication work similarly as in definition 3.3.1. Unlike BFV however, CKKS works with different moduli q_L at each level L. This also casts off the need for up- and downscaling by δ when multiplying ciphertexts. The CKKS.ReLin operation serves the same purpose as in BFV, the rescaling operation is new however and takes care of the scale management. CKKS.ReScale can be employed whenever we want to work with ciphertexts at different levels, modifying a given ciphertext to the scale of the other enables the other operations to work just as usual. Figure 3.2 shows the extended course of action in CKKS with a preceeding encoding and decoding step.

Table 3.2: Summary of the parameters and symbols in CKKS.

Symbol	Space	Explanation
λ	$\in \mathbb{R}$	Security parameter
d	$\in \mathbb{N}$	Index of the cyclotomic polynomial used in R
P	$\in \mathbb{Z}$	Factor used during relinearisation
h	$\in \mathbb{Z}$	Hamming weight of the secret key (used by χ_{key})
σ	$\in \mathbb{R}$	Standard deviation of the Gaussian χ_{error}
q_L	$\in \mathbb{N}$	Modulus of $R/q_L R$ at level L
δ	$\in \mathbb{N}$	Scaling factor used when encoding
δ^{-1}	$\in \mathbb{R}$	Inversion coefficient of the effect of δ
s	$\in \{0, \pm 1\}^N$	Secret Key
$\boldsymbol{p}$	$\in (R/q_L R)^2$	Public Key (b, a)
$\boldsymbol{\gamma}$	$\in (R/(Pq_L)R)^2$	Relinearisation Key
$\boldsymbol{z}$	$\in \mathbb{C}^{N/2}$	Plain input vector
m	$\in R$	Plaintext Message
$\boldsymbol{c}$	$\in (R/q_L R)^2$	Ciphertext Message
$\bar{\boldsymbol{c}}$	$\in (R/q_L R)^3$	Slightly larger ciphertext from multiplication

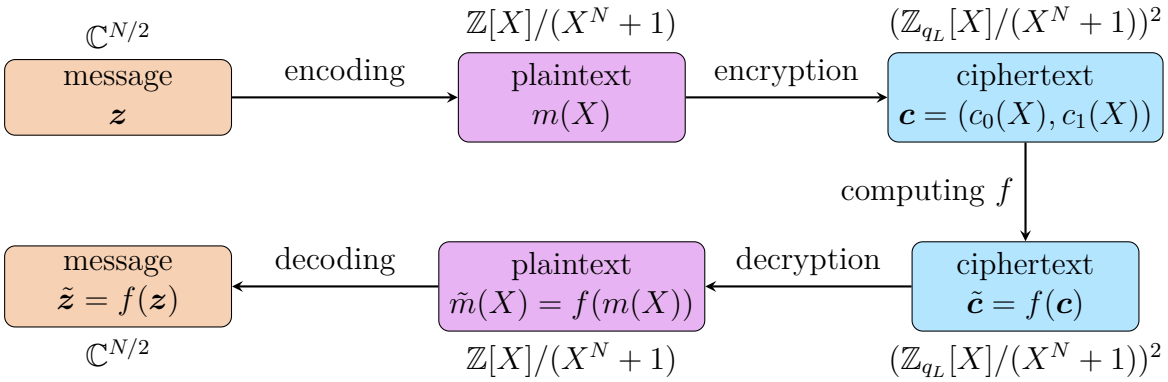

Figure 3.2: Schematic overview of CKKS, adapted from Huynh 2020. A plain vector $\boldsymbol{z} \in \mathbb{C}^{N/2}$ is encoded to a plaintext polynomial $m = \text{CKKS.Encode}(\boldsymbol{z})$, encrypted to the ciphertext $\boldsymbol{c} = \text{CKKS.Encrypt}(\boldsymbol{p}, m)$ using the public key $\boldsymbol{p}$, operated on using a combination of CKKS.{Add, Mult, ReLin, ReScale} ciphertext operations and finally decrypted and decoded to a new $\tilde{\boldsymbol{z}} = \text{CKKS.Decode}(\text{CKKS.Decrypt}(s, \tilde{\boldsymbol{c}}))$ using the secret key s.

3.4.3 Verification of the Additive Homomorphism

3.4.1 Theorem: CKKS encryption is homomorphic with respect to addition

CKKS.Encode and CKKS.Encrypt should encrypt in such a way that the addition algebra can be retained even in the transformed space, showing that we can indeed refer to it as homomorphic encryption.

Proof. Similar to the BFV scheme proof (theorem 3.3.1), we aim to show that two input vectors $\boldsymbol{z}, \boldsymbol{z}' \in \mathbb{C}^{N/2}$ can be encoded, encrypted and added - and finally decrypted back to $\overline{\boldsymbol{z}} = \boldsymbol{z} + \boldsymbol{z}'$.

Due to the extremely high similarity of the BFV and CKKS schemes, they are even identical in their encryption, decryption and adding procedures, the only thing that remains to be shown is the additivity (or even linearity) of CKKS.Encode.

Encoding $\boldsymbol{z}$ and $\boldsymbol{z}'$ into m and m', we obtain

$$m := \text{CKKS.Encode}(\boldsymbol{z}) = (\underline{\sigma}^{-1} \circ \underline{\rho_\delta}^{-1} \circ \underline{\pi}^{-1})(\boldsymbol{z})$$

comprised of three transformations $\underline{\sigma}^{-1}$, $\underline{\rho_\delta}^{-1}$ and $\underline{\pi}^{-1}$ which can be studied separately for their approximate additivity. If a function is linear and bijective (turning it into an isomorphism), its inverse will also be linear. We will utilize this below by only showing the additivity of $\underline{\sigma}$, $\underline{\rho_\delta}$ and $\underline{\pi}$, assuming their (approximate) bijectivity. Especially the bijectivity of $\underline{\sigma}$ is cumbersome to show and for more details we refer the reader to Cheon et al. 2017.

- The canonical embedding $\underline{\sigma}$ evaluates an input polynomial on the N^{th} roots of unity $\{\xi_j\}_{j\in\mathbb{Z}_d^*}$. For any two polynomials $p_1, p_2 \in \mathcal{S}$,

$$\underline{\sigma}(p_1 + p_2) = \Big((p_1 + p_2)(\xi_j)\Big)_{j\in\mathbb{Z}_d^*} = \Big(p_1(\xi_j) + p_2(\xi_j)\Big)_{j\in\mathbb{Z}_d^*} = \underline{\sigma}(p_1) + \underline{\sigma}(p_2)\,.$$

- The rounding operation $\underline{\rho_\delta}^{-1}$ is only approximately additive due to its nature [4]. For any two vectors $\boldsymbol{h_1}, \boldsymbol{h_2} \in \mathbb{H}$,

$$\begin{aligned}\underline{\rho_\delta}^{-1}(\boldsymbol{h_1} + \boldsymbol{h_2}) &= \lfloor \delta \cdot (\boldsymbol{h_1} + \boldsymbol{h_2}) \rceil_{\underline{\sigma}(R)} = \lfloor \delta\boldsymbol{h_1} + \delta\boldsymbol{h_2} \rceil_{\underline{\sigma}(R)} \approx \lfloor \delta\boldsymbol{h_1} \rceil_{\underline{\sigma}(R)} + \lfloor \delta\boldsymbol{h_2} \rceil_{\underline{\sigma}(R)} \\ &\approx \underline{\rho_\delta}^{-1}(\boldsymbol{h_1}) + \underline{\rho_\delta}^{-1}(\boldsymbol{h_2})\,.\end{aligned}$$

  Its inverse $\underline{\rho_\delta}$ is fully additive nevertheless, since it acts as the identity (up to a scalar factor) of the subset $\underline{\sigma}(R)$ back to an element of $\mathbb{H}$.

- The natural projection $\underline{\pi}$ halves a vector in $\mathbb{H}$ to an element of $\mathbb{C}^{N/2}$ which is naturally linear. Consider any $\boldsymbol{h_1}, \boldsymbol{h_2} \in \mathbb{H}$, then

$$\underline{\pi}(\boldsymbol{h_1} + \boldsymbol{h_2}) = (h_{1j} + h_{2j})_{j\in T} = (h_{1j})_{j\in T} + (h_{2j})_{j\in T} = \underline{\pi}(\boldsymbol{h_1}) + \underline{\pi}(\boldsymbol{h_2})\,.$$

As every step in the full encoding process $\underline{\sigma}^{-1} \circ \underline{\rho_\delta}^{-1} \circ \underline{\pi}^{-1}$ is additive, CKKS.Encode indeed acts additively. CKKS.Decode on the other hand is only approximately additive due to the rounding operation required in between.

The rest follows from theorem 3.3.1 as encryption and addition of the BFV scheme are identical. All in all for CKKS, using the secret key s and public key $\boldsymbol{p}$,

$$\text{Decode}(\text{Decrypt}(s, \text{Add}(\text{Encrypt}(\boldsymbol{p}, \text{Encode}(\boldsymbol{z})), \text{Encrypt}(\boldsymbol{p}, \text{Encode}(\boldsymbol{z}'))))) \approx \boldsymbol{z} + \boldsymbol{z}'\,.$$

We can conclude that encoding *and* encryption in CKKS are indeed homomorphic with respect to addition. □

As the public key $\boldsymbol{p} = (b, a)$ corresponds to a sample from the RLWE distribution (corollary 2.2.1), the implied security of the CKKS scheme is given by the hardness assumption of LWE (theorem 2.2.1). An attacker trying to decrypt a ciphertext $\boldsymbol{c}$, given only the public key $\boldsymbol{p}$, would thereby need to solve the RLWE search problem (corollary 2.2.2) which is known to be hard (Lyubashevsky, Peikert and Regev 2010).

Microsoft SEAL 4.0 2022 implements the scheme, enabled using `seal::scheme_type::ckks`.

[4] For an illustrative counterexample of the additivity of rounding, refer to https://math.stackexchange.com/questions/58239/linear-functions-with-rounding.

Chapter 4

Implementation

4.1 Chosen Software Architecture

In the given setting, the most accessible frontend is commonly a JavaScript web application. A web-based demonstrator to show how to classify handwritten digits when using homomorphic encryption was implemented, comprised of a C++ server and a React[1] frontend, confer figure 1.1.

To still make the classification run as quickly and efficiently as possible, a C++ binary runs in the backend providing an HTTP API to the frontend application. In order to allow for more flexibility of the HTTP server, the initial approach was to pipe requests through a dedicated web application framework with database access that would allow, for instance, user management next to the basic classification. However, the resulting communication and computation overhead, even when running with efficient protocols such as ZeroMQ, was too high.

Extending the accessibility argument to reproducibility, Docker is a solid choice (Nüst et al. 2020). The deployment is structured into two Docker images, *classifier* and *frontend*, easily scalable to multiple instance of the C++ upstream server using a round-robin load-balancing strategy of the single reverse proxy Nginx[2].

To run the attached demo project, simply execute

```
docker-compose build
docker-compose up
```

in the `code` folder and point your browser to `https://localhost`.

Using a Docker Multi-Stage Build, the application images were optimized towards a zero-dependency Alpine Linux image which contains nothing but compiled binaries and linked libraries. This is achieved by introducing intermediate layers including all necessary compiler libraries and dependencies and only copying the resulting binary to the final image. Similarly, the *frontend* build process of course requires Node JS, a common JavaScript engine used for the React compilation step, in a previous build layer. Yet, the final image only serves static files without any further server logic required and thus omits the entire JavaScript engine and associated libraries for the image. Details on the build process can be found in `code/classifier/classifier.Dockerfile` and `code/frontend/frontend.Dockerfile`.

[1] https://reactjs.org/
[2] http://nginx.org/

4.2 The MNIST dataset

The Modified National Institute of Standards and Technology (MNIST) dataset of handwritten digits (LeCun and Cortes 1998) contains 60,000 train and 10,000 test images with corresponding labels. Some sample images are displayed in figure 4.1, with ascending labels from 0 to 9. In order to stick to the traditional feedforward technique with data represented in vector format, therefore it is common to reshape data from $(28, 28)$ images (represented as grayscale values in a matrix) into a 784 element vector.

Figure 4.1: Sample images of the MNIST dataset of handwritten digits (LeCun and Cortes 1998). The dataset contains 70,000 images of 28×28 grayscale pixels valued from 0 to 255 as well as associated labels (as required for supervised learning).

MNIST is one of the most commonly used datasets in Machine Learning, featured in an abundant number of tutorials and showcases, all in all it is very well studied. The National Institute of Standards and Technology recently published an extended version with uppercase and lowercase letters of the Latin alphabet contained as well (EMNIST), processed in the same way as MNIST, which should also work with our demonstrator.

4.3 Our Neural Network

The neural network implemented in our demonstrator was trained using the unencrypted standard MNIST dataset of 60,000 images, split into 90 % training and 10 % validation data. The training process itself was performed using the *Tensorflow* machine learning framework in Python [3]. The implemented network then has the following layer structure (also confer figure 2.4):

$$\text{Layer 1: } \boldsymbol{h} = \text{relu\_taylor}(M_1\boldsymbol{x} + \boldsymbol{b_1})$$
$$\text{Layer 2: } \boldsymbol{y} = \text{softmax}(M_2\boldsymbol{h} + \boldsymbol{b_2})$$

Expressed in Python code, using the *Keras* extension of Tensorflow,

```
import tensorflow as tf

model = tf.keras.Sequential([
  tf.keras.layers.Flatten(input_shape=(28, 28)),
  tf.keras.layers.Dense(128, activation=relu_taylor),
  tf.keras.layers.Dense(10),
  tf.keras.layers.Activation(tf.keras.activations.softmax),
])
```

[3] https://www.tensorflow.org/

For performance metrics and some statistical analysis of the network's accuracy, refer to section 5.2.

To gain some intuition on what the two layers look like internally, the following plots of weights and biases have been made:

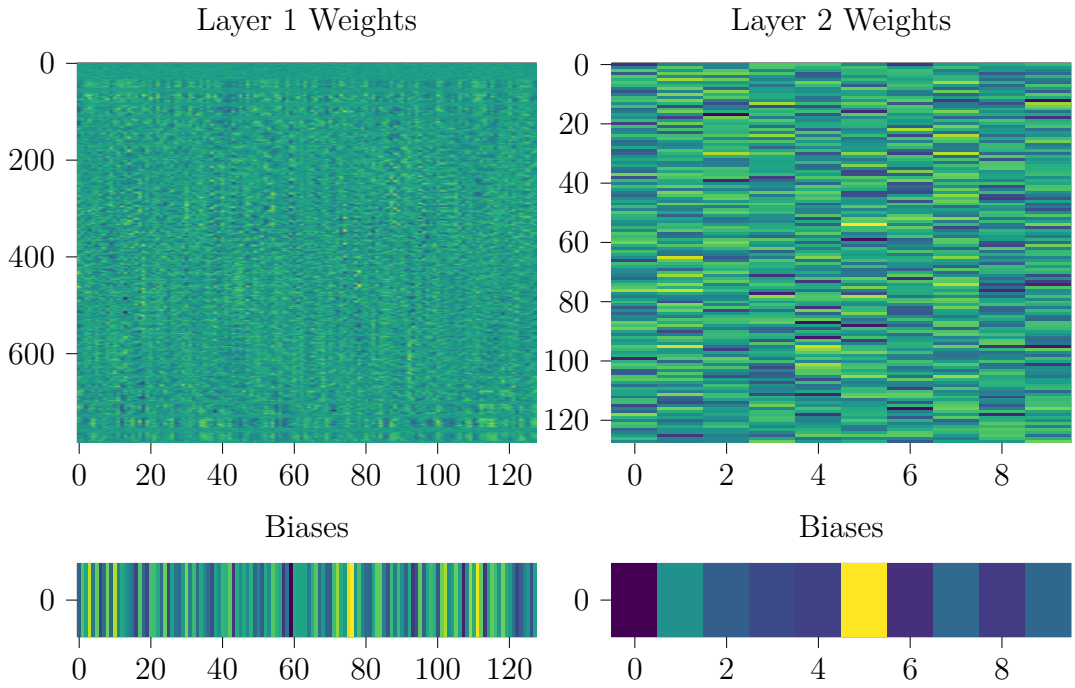

Figure 4.2: First and Second Layer Weights and Biases of the trained neural network. The weight matrices (784×128 and 128×10) are skewed to account for the different dimensions used. The biases have the same shape as the output of the matrix multiplication and the input of the next layer.

After going through both layers (confer figure 4.2), with the approximative relu_taylor activation function in between, the second (last) layer of the network outputs a vector of 10 scalars, each corresponding to one digit from 0 to 9. When finally applying the softmax function to the output, we can interpret the values as probabilities for each digit.

4.4 Matrix-Vector Multiplication

The dot product that is required as part of the neural network evaluation process needs to be implemented on SEAL ciphertexts as well.

There are multiple methods to achieve a syntactically correct dot product (matrix-vector multiplication) as described by Juvekar, Vaikuntanathan and Chandrakasan (2018) for (square) matrices.

1. **Naïve MatMul** - simple to derive but impractical in practice due to the limited further applicability of the result consisting of multiple ciphertexts. Applicable to arbitrary matrix dimensions, i.e. matrices $M \in \mathbb{R}^{s\times t}$, of course limited by the unreasonably high memory consumption and computation time of this approach.
2. **Diagonal MatMul** - a simple and practical solution applicable to square matrices $M \in \mathbb{R}^{t\times t}$ that has a major advantage compared to the previous method as the computation yields a single ciphertext object instead of many which can be directly passed on to a following evaluation operation.
3. **Hybrid MatMul** - essentially extending the diagonal method by generalising the definition of the diagonal extraction mechanism to 'wrap around' in order to match the dimensionality of the input vector. Applicable to arbitrary matrix dimensions, i.e. matrices $M \in \mathbb{R}^{s\times t}$ and favourable compared to the Naïve Method.
4. **Babystep-Giantstep MatMul** - a more sophisticated technique aiming to significantly reduce the number of Galois rotations as they are rather expensive to carry out, with a performance boost especially noticeable for higher matrix dimensions. Without further modification, applicable to square matrices.

For the following, define

$$\begin{aligned}\mathrm{rot}_j : \mathbb{R}^t \mapsto \mathbb{R}^t,\ \{\mathrm{rot}_j(\boldsymbol{x})\}_i &= x_{i+j}\\ \mathrm{diag}_j : \mathbb{R}^{t\times t} \mapsto \mathbb{R}^t,\ \{\mathrm{diag}_j(M)\}_i &= M_{i,(i+j)}\end{aligned}$$

with all indices $i, j \in \mathbb{Z}_t$ member of the cyclic quotient group $\mathbb{Z}_t := \mathbb{Z}/t\mathbb{Z}$ of all integers modulo t, meaning that overflowing indices simply wrap around again starting at index 0 to simplify notation. For the sake of compactness, we stick to this notation for the rest of the section.

4.4.1 The Naïve Method

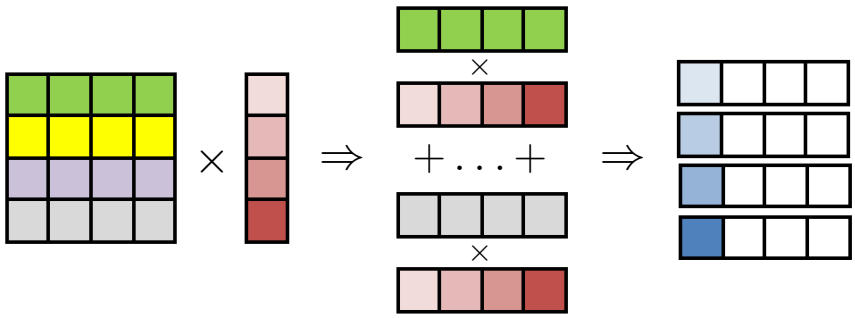

Figure 4.3: The naïve method to multiply a square matrix with a vector (adapted from Juvekar, Vaikuntanathan and Chandrakasan 2018).

Term by term, one can express a matrix-vector product of $M \in \mathbb{R}^{s \times t}$ and $\boldsymbol{x} \in \mathbb{R}^s$ as follows (also see figure 4.3):

$$\{M\boldsymbol{x}\}_i = \sum_{j=1}^{t} M_{ij} x_j \,.$$

Accordingly, a natural (or rather, naïve) way to model this multiplication in Microsoft SEAL would be to

1. encode each i-th matrix row $(M_{i,1}, M_{i,2}, ..., M_{i,t})$ using the `Encoder` with matching parameters to the ciphertext of the encoded vector $\boldsymbol{x}$.
2. multiply each encoded row with the encrypted vector using `Evaluator.multiply_plain()` to obtain the ciphertext vector $\boldsymbol{y_i} \in \mathbb{R}^s$ for row i.
3. perform the 'rotate-and-sum' algorithm (Juvekar, Vaikuntanathan and Chandrakasan 2018) on each resulting vector (ciphertext) $\boldsymbol{y_i}$ to obtain the actual dot product of the matrix row with the vector $\boldsymbol{x}$:
   (a) using Galois automorphisms, rotate the entries of $\boldsymbol{y_i}$ by $\frac{s}{2}$ elements to obtain $\text{rot}_{\frac{s}{2}}(\boldsymbol{y_i})$.
   (b) perform an element-wise sum $\boldsymbol{y_i} + \text{rot}_{\frac{s}{2}}(\boldsymbol{y_i})$ whose first (and also second) half now contains the sum of the two halves of $\boldsymbol{y_i}$.
   (c) repeat the previous two steps $\log_2(s)$ times, halving the split parameter s each time until one obtains 1 element, which yields us the requested sum of all entries $\sum_{k=1}^{s}\{\boldsymbol{y_i}\}_k$ as the dot product of $\boldsymbol{x}$ and $\boldsymbol{y_i}$.
4. Given all the 'scalar' results of each row-vector dot product, we can construct the resulting matrix-vector product.

Adapting to non-square matrices The weight matrices in the given classification setting are not at all square, on the contrary their output dimension tends to be much lower than the input dimension as the overall goal is to reduce it from $28^2 = 784$ down to 10.

However, that also means one cannot directly apply the naïve or diagonal methods for multiplication. This 'flaw' can be mitigated by a simple zero-padding approach in order to make the matrix square, filling in zeroes until the lower-sized dimension reaches the higher one.

4.4.2 The Diagonal Method

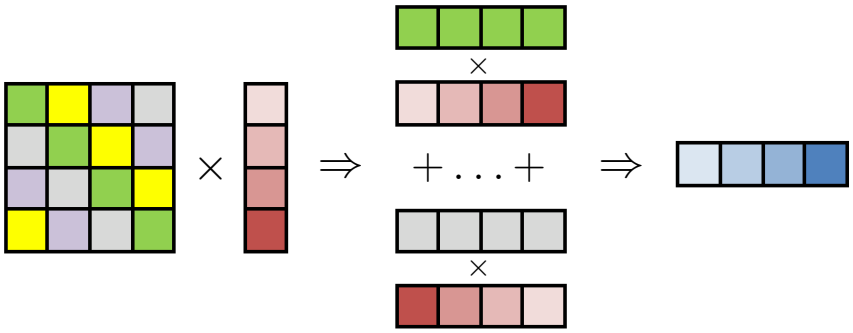

Figure 4.4: The diagonal method to multiply a square matrix with a vector (adapted from Juvekar, Vaikuntanathan and Chandrakasan 2018).

As can be seen in figure 4.4, we perform the vector-vector products over the diagonals of the matrix instead of the rows and rotate $\boldsymbol{x}$ by one for each rotation.

4.4.1 Theorem: Diagonal Method

Given a matrix $M \in \mathbb{R}^{t \times t}$ and a vector $\boldsymbol{x} \in \mathbb{R}^t$, the dot product between the two can be expressed as

$$M\boldsymbol{x} = \sum_{j=0}^{t-1} \mathrm{diag}_j(M) \cdot \mathrm{rot}_j(\boldsymbol{x}) \,.$$

Proof. For all indices $i \in \mathbb{Z}/t\mathbb{Z}$,

$$\left\{ \sum_{j=0}^{t-1} \mathrm{diag}_j(M) \cdot \mathrm{rot}_j(\boldsymbol{x}) \right\}_i = \sum_{j=0}^{t-1} M_{i,(i+j)} x_{i+j} \overset{[k=i+j]}{=} \sum_{k=i}^{t+i-1} M_{ik} x_k = \sum_{k=0}^{t-1} M_{ik} x_k = \{M\boldsymbol{x}\}_i \,.$$

□

The key idea of this optimization is to exploit the Single Instruction Multiple Data (SIMD) structure of the encryption schemes, in particular that of CKKS, and aggregating the result in one of the ciphertext objects.

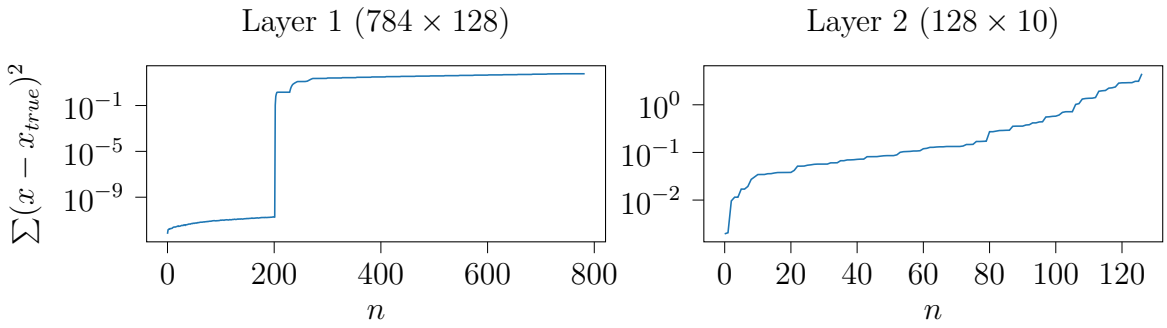

Figure 4.5: Diagonal Method error development after each rotation of the input vector.

One major problem of the diagonal method is that it requires many Galois rotations of $\boldsymbol{x}$, which is slow and also causes a large error after too many consecutive rotations (confer figure 4.5).

4.4.3 The Hybrid Method

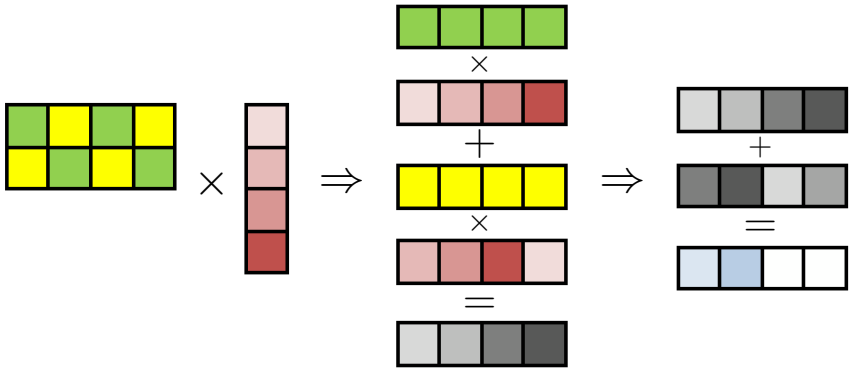

Figure 4.6: The hybrid method to multiply an arbitrarily sized matrix with a vector (adapted from Juvekar, Vaikuntanathan and Chandrakasan 2018).

To further extend the previous matrix multiplication method to solve the problem (cf. section 4.4.1), it is first necessary to extend the definition of the diag operator to non-square matrices $M \in \mathbb{R}^{s\times t}$. For the following, extending the above definition:

$$\mathrm{diag}_j : \mathbb{R}^{s\times t} \mapsto \mathbb{R}^t,\ \{\mathrm{diag}_j(M)\}_i = M_{i,(i+j)}\,.$$

4.4.2 Theorem: Hybrid Method

For a matrix $M \in \mathbb{R}^{s\times t}$ with t a whole multiple of s and a vector $\boldsymbol{x} \in \mathbb{R}^t$,

$$M\boldsymbol{x} = (y_i)_{i\in\mathbb{Z}/s\mathbb{Z}} \text{ with } \boldsymbol{y} = \sum_{k=1}^{t/s} \mathrm{rot}_{ks}\left(\sum_{j=1}^{s} \mathrm{diag}_j(M)\cdot \mathrm{rot}_j(\boldsymbol{x})\right).$$

Proof. For all indices $i \in \mathbb{Z}/s\mathbb{Z}$,

$$\{\boldsymbol{y}\}_i = \left\{\sum_{k=1}^{t/s} \mathrm{rot}_{ks}\left(\sum_{j=1}^{s} \mathrm{diag}_j(M)\cdot \mathrm{rot}_j(\boldsymbol{x})\right)\right\}_i = \sum_{k=1}^{t/s}\sum_{j=1}^{s} M_{i,(i+j)+ks}\,x_{(i+j)+ks}\,,$$

substituting $l = i+j+ks$ and condensing the nested sums into one single summation expression since $\sum_{k=1}^{t/s}\sum_{j=1}^{s} f(j+ks) = \sum_{l=1}^{t} f(l)$, we obtain

$$y_i = \sum_{l=1+i}^{t+i} M_{il}x_l = \sum_{l=1}^{t} M_{il}x_l = \{M\boldsymbol{x}\}_i\,.$$

For a longer example on the index notation and derivation of the terms above including the condensed sum, refer to appendix A.2. □

Due to its low number of operations, the hybrid method almost always outperforms the naïve and diagonal methods (Juvekar, Vaikuntanathan and Chandrakasan 2018). A schematic representation illustrating the process can be seen in figure 4.6.

To exemplarily discuss the implementation of an HE algorithm, we break down the following piece of code responsible for the hybrid matrix multiplication. Thanks to SEAL's object-oriented

interface and explicit, consistent naming, the code snippets are mostly self-explanatory in combination with some additional comments.

We first encode the matrix diagonals using the `seal::CKKSEncoder` into a vector of plaintexts (each containing the information of one diagonal).

```
// diagonal method preparation
size_t in_dim = matrix.shape(0), out_dim = matrix.shape(1);
std::vector<seal::Plaintext> diagonals = encodeMatrixDiagonals(matrix,
↪  encoder, evaluator, in_out.parms_id(), in_out.scale(), nullptr, OUT_DIM);
```

Once this is done, we evaluate the inner sum $\sum_{j=1}^{s} \mathrm{diag}_j(M) \cdot \mathrm{rot}_j(\boldsymbol{x})$ using a loop.

```
// perform the actual multiplication
seal::Ciphertext sum = in_out;  // makes a copy
evaluator.multiply_plain_inplace(sum, diagonals[0]);  // performs the first
↪  vector-vector product
for (auto offset = 1ULL; offset < in_dim; offset++) {
  seal::Ciphertext tmp;  // for all remaining offsets:
  evaluator.rotate_vector_inplace(in_out, 1, galois_keys);
  evaluator.multiply_plain(in_out, diagonals[offset], tmp);
  evaluator.add_inplace(sum, tmp);
}
in_out = sum;  // and we arrive at the first result
evaluator.rescale_to_next_inplace(in_out);  // scale down once
```

Finally, we exploit the repetitions in the resulting sum from above and rotate t/s times to end up with the sum of all chunks, encoded in one final ciphertext vector.

```
// perform the rotate-and-sum algorithm
seal::Ciphertext rotated = in_out; // makes a copy
for (size_t chunk = 0; chunk < in_dim / out_dim; chunk++) {
  evaluator.rotate_vector_inplace(rotated, out_dim, galois_keys);
  evaluator.add_inplace(in_out, rotated);  // adds rotated result to itself
}
return in_out;
```

In the Machine Learning context, it is common to have a much higher input dimension than output dimension, usually leading to fully connected layers with matrices $M \in \mathbb{R}^{s \times t}$ with $s \ll t$. The diagonal method is especially efficient in these cases as it only requires $s + \frac{t}{s} = \frac{s^2+t}{s}$ rotations and s multiplications.

As outlined in section 5.3, the hybrid method will prove to be the fastest method for the matrix sizes in our given project, with the 2nd best numerical accuracy.

4.4.4 The Babystep-Giantstep Method

Since Galois rotations are the most computationally intensive operations in most cryptographic schemes used today (Dobraunig et al. 2021), they take a large toll on the efficiency. In order to reduce the number of rotations required, one can make use of the Babystep-Giantstep (BSGS) optimisation as described in Halevi and Shoup 2018, which works as follows:

4.4.3 Theorem: Babystep-Giantstep Method

Given a matrix $M \in \mathbb{R}^{t\times t}$ and a vector $\boldsymbol{x} \in \mathbb{R}^t$, with $t = t_1 \cdot t_2$ split into two BSGS parameters $t_1, t_2 \in \mathbb{N}$ and

$$\text{diag}'_p(M) = \text{rot}_{-\lfloor p/t_1 \rfloor \cdot t_1}(\text{diag}_p(M)),$$

one can express a matrix-vector multiplication as follows:

$$M\boldsymbol{x} = \sum_{k=0}^{t_2-1} \text{rot}_{(kt_1)}\left(\sum_{j=0}^{t_1-1} \text{diag}'_{(kt_1+j)}(M) \cdot \text{rot}_j(\boldsymbol{x})\right)$$

where $\cdot$ denotes an element-wise multiplication of two vectors.

A proof of the above theorem can be found in appendix A.2.

Note that the optimized matrix-vector multiplication only requires $t_1 + t_2$ rotations as we can store the t_1 inner rotations of the vector $\boldsymbol{x}$ for the upcoming evaluations. For larger matrices and vectors (larger t), $t_1 + t_2$ are indeed much smaller than the conventional number of required rotations $t = t_1 \cdot t_2$ in the diagonal method, or $\frac{s^2+t}{s}$ rotations in the hybrid method, which was the point of this modification in the first place. However, the number of multiplications and additions remains high - at least t multiplications are required, whereas the hybrid method only requires s multiplications (potentially much lower than t).

As we will see in section 5.3, the BSGS method also improves the performance of our classification process compared to the diagonal method, yet for the chosen parameters it does not reach the speed of the hybrid method. the approach of splitting the sum into two parts improves its performance close to that of the hybrid method.

4.5 Polynomial Evaluation

As the encryption hides the true value, we cannot directly evaluate the relu function since we have no way of telling whether it is larger than 0 or not. Using a finite series we can approximate the function though, also in the encrypted domain, because we can leverage the addition and multiplication operations of CKKS.

Finding a such approximation is not particularly hard, Taylor's theorem provides us with an explicit method to approximate a given analytic function in this way:

$$T_N f(x, x_0) := \sum_{n=0}^{N} \frac{f^{(n)}(x_0)}{n!}(x - x_0)^n$$

To accomplish the best possible result however, a Chebyshev interpolation targeted at the corresponding domain subset may be a more suitable choice. Performing such an interpolation

on the interval $[-5, 10] \subset \mathbb{R}$ around 0 yields us the polynomial

$$\text{relu\_taylor}(x) = -0.006137x^3 + 0.090189x^2 + 0.59579x + 0.54738$$

which is plotted next to the function it is supposed to interpolate in figure 4.7.

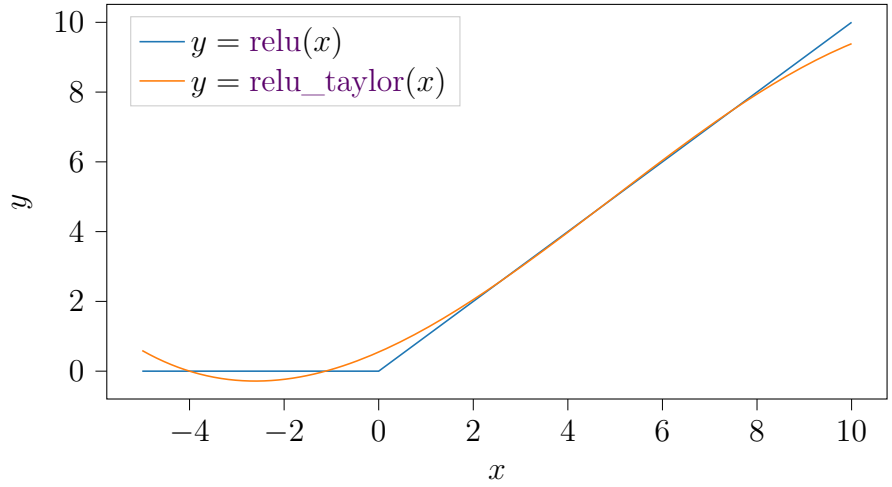

Figure 4.7: Comparison of the $\text{relu}(x)$ activation function vs. its series approximation $\text{relu\_taylor}(x)$, plotted on the given domain. Outside of it, the two functions strongly disagree.

Next, we want to implement this polynomial evaluation using SEAL. From the implementation perspective, there are three properties to keep in mind when operating on a SEAL ciphertext (`seal::Ciphertext x`):

1. Scale (retrieved using `x.scale()`)
   Can be adjusted with: `evaluator.rescale_inplace()`
2. Encryption Parameters (retrieved using `x.parms_id()`)
   Can be adjusted with: `evaluator.mod_switch_to_inplace()`
3. Ciphertext Size (retrieved using `x.size()`)
   Can be adjusted with: `evaluator.relinearize_inplace()`

For addition, the scales must be the same and they luckily will not change after the operation. The more delicate operation is ciphertext multiplication. Each time one multiplies two ciphertexts, the scales multiply (logarithmically, they add up, i.e. the common representations in bits are added together). The chain index reduces by 1, which for an encoded ciphertext depends on the coeff moduli. There must be enough bits remaining to perform the multiplication, namely $\log_2(scale)$ bits.

To illustrate the connections of these properties to one another, the following explanation of Wei Dai, one of the maintainers of SEAL, on the "Scale out of bounds" error gives some good insight:

> Scale has nothing to do with noise. "Scale out of bounds" can appear even if noise is extremely low. Although repeated multiplication of a ciphertext by a plaintext will slowly increase the noise, it is not the reason why you see "scale out of bounds".
>
> The "Scale out of bounds" error specifically means that the scale of a ciphertext or plaintext is larger than the product of all elements in `coeff_modulus`. If you perform multiplications without rescaling, you can quickly see this error.

> The more rescaling you perform, the less elements will be left in `coeff_modulus`. Even if you managed to have the same scale in a ciphertext after every multiplication and rescale, eventually the `coeff_modulus` can be too small to accommodate another multiplication (Dai 2020).

When evaluating a polynomial in SEAL, the above considerations need to be kept in mind when encoding the coefficients, multiplying the ciphertext $\boldsymbol{x}$ with itself to reach higher powers and adding together the weighted monomials. We of course leverage the SIMD structure of the encryption scheme in order to turn the computation into an element-wise polynomial evaluation of the 1st layer's output (an encrypted vector) before passing it on to the 2nd layer.

4.6 Further Implementation Challenges

When performing arbitrary computations on a ciphertext in SEAL, it is possible to encounter a *transparent ciphertext* from time to time. That is a ciphertext identically equal to 0 (mathematically, the tuple's second polynomial is zero, confer definition 3.4.4), and it is usually not considered a valid encryption as anyone who has it can immediately 'decrypt' it to its underlying value of 0. However, for intermediate values of the computation at hand, forwading values from addition to multiplication multiple times in our network, this is not an issue as long as we do not send the value back to the client, i.e. expose its internal structure (Laine 2020).

In our usual setting of a web-based demonstrator for recognising handwritten digits, this situation cannot be avoided - but as long as the client does not send a ciphertext identical to 0, our final classification result (a vector of 10 elements) will never be 0. Therefore, the server binary is compiled with the `-DSEAL_THROW_ON_TRANSPARENT_CIPHERTEXT=OFF` flag enabled, preventing a system halt in the case of an intermediary value evaluating to 0.

An important optimisation was to pre-encode the weight matrices and bias vectors upon startup of the server. This halved the individual request-response times, especially for the fast BSGS and hybrid methods.

The first layer multiplication is much slower than the second-layer one due to the large matrices, depending on the multiplication method, but around a factor of 60-100. For more details on runtime benchmarks, refer to section 5.3.

Chapter 5

Results

5.1 The Training Process

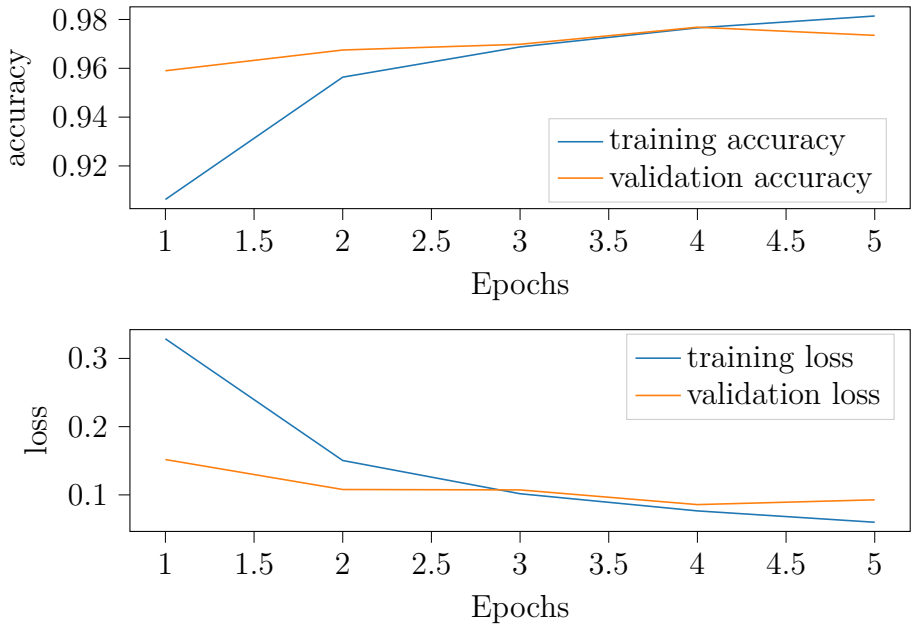

Figure 5.1: Development of the classification accuracy and the mean squared error during the training process of our neural network. Training and validation set metrics are plotted separately. When the validation accuracy starts to drop, the training process halts with the next epoch to prevent overfitting.

The machine learning framework behind the project, Tensorflow, splits its training process into *epochs*, which can be found on the x-axis in the plot above. For each training epoch, we find the progress that has been made in a single epoch by looking at the new accuracy (which percentage of the images has been classified correctly) and the loss function (MSE in this case). Per training run, we make a differentiation between training metrics and validation metrics, illustratively shown above for the given network. The validation data is not involved with the training process, it is only used to find a point in the process when training accuracy still rises while validation accuracy starts to drop (confer figure 5.1). At this point we will likely find the network's learning process in an *overfitting* situation, so the training process terminates.

5.2 Accuracy, Precision, Recall

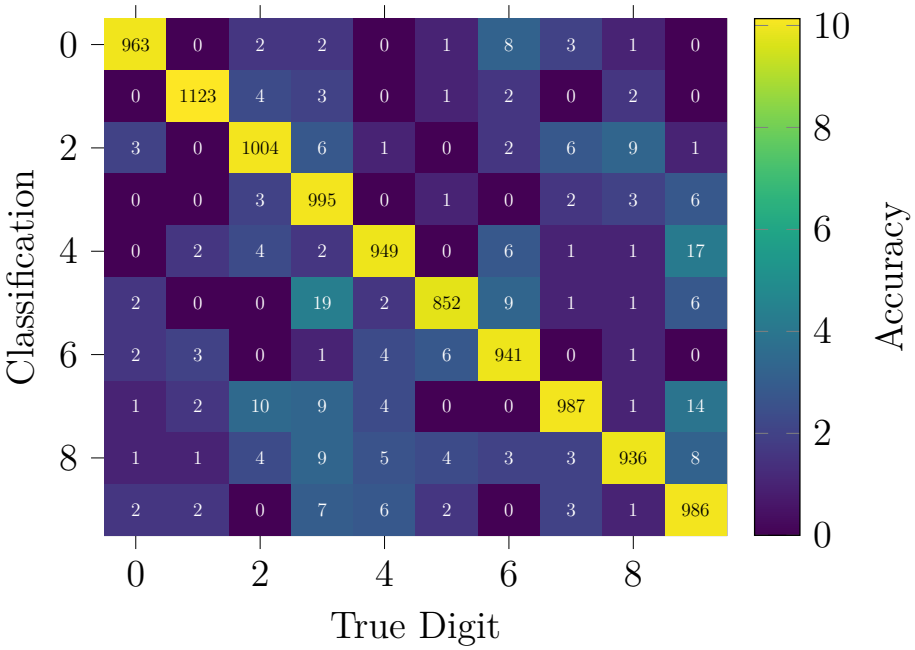

Figure 5.2: The Confusion Matrix of the trained network, showing digit-wise correct classifications in the diagonal and misclassifications, per digit-pair, in the off-diagonals. The matrix values were visually enhanced by mapping them to their logarithm base 2.

As we can see in figure 5.2, the majority of all images are classified correctly (visible in the diagonal). What makes the confusion matrix so interesting is identifying frequently mixed up digits, for instance, 3 and 5, 2 and 7 or 4 and 9. Judging with a human eye, this is somewhat reasonable, even more so when looking at the actual set of misclassified images (figure 5.3).

Figure 5.3: MNIST test images with true labels $0, 1, 2, 3, 4, 5, 6, 7, 8, 9$ that were misclassified as $6, 8, 9, 8, 2, 6, 0, 9, 2, 3$ by the neural network.

The plain network classifies 97.62 % of the 10,000 test images correctly. Running the encrypted classification on the full test set too, the encrypted network classifies 97.31 % of the test images correctly in $3\frac{1}{2}$ hours at full CPU utilisation, using the hybrid matrix multiplication method. For a binary classification, two further metrics of interest are

$$\text{Precision} = \frac{\text{tp}}{\text{tp} + \text{fp}} \qquad \text{Recall} = \frac{\text{tp}}{\text{tp} + \text{fn}}$$

with tp ... True Positives, fp ... False Positives, fn ... False Negatives.

Precision (also referred to as PPV, positive predictive value) refers to the ability of the network to classify positive samples correctly, while Recall explains the completeness of the classified samples (i.e. how few true positives have been left out).

Table 5.1: Precision and Recall of the trained network for each digit individually, above for the plain network evaluation (P) and below for the encrypted evaluation (E).

Digit	0	1	2	3	4	5	6	7	8	9
Precision (P)	0.978	0.990	0.959	0.960	0.985	0.968	0.977	0.976	0.963	0.978
Recall (P)	0.986	0.989	0.975	0.977	0.975	0.964	0.980	0.964	0.967	0.955
Precision (E)	0.987	0.976	0.979	0.946	0.961	0.960	0.981	0.974	0.975	0.956
Recall (E)	0.989	0.990	0.958	0.981	0.975	0.966	0.972	0.963	0.937	0.959

Averaged over all digits, the mean precision (in plain) amounts to 97.37 % while the average recall is similarly high at 97.36 %. The encrypted network evaluation of the full test set yields an average Mean Max-Relative Error (see table 5.2) of 2.97 % using the hybrid method. And although it is numerically less accurate than the plain computation, only a handful of the 10,000 images were classified incorrectly, that the plain network managed to classify correctly.

5.3 Performance Benchmarks

This section finally gives a runtime and communication overhead analysis of the project. For fair comparisons, the preparations required for each method individually were not taken into account, as they can be performed once at the beginning of the program.

Table 5.2: Performance benchmarks and communication overhead of the classification procedure on an Intel® i7-5600U CPU, including the encoding and decoding steps. Different parameter sets $\boldsymbol{B_1}, \boldsymbol{B_2}, \boldsymbol{N}$ are compared for each of the implemented matrix multiplication methods *diagonal*, *hybrid* and *Babystep-Giantstep* (BSGS), looking at the averaged runtime, message size and also the accuracy when compared to the plain result ($\boldsymbol{\Delta}$).

$\boldsymbol{B_1}$ ... Coefficient Moduli start bits (also equal to the last)
$\boldsymbol{B_2}$ ... Coefficient Moduli middle bits, also defines the scale as 2^{B_2}
$\boldsymbol{N}$ ... Polynomial Modulus Degree, found in the exponent of $p(X) = X^N + 1$
$\boldsymbol{T}$ ... Runtime of encryption + classification + decryption
$\boldsymbol{M}$ ... Message Size (Relin Keys + Galois Keys + Request Ciphertext + Response Ciphertext)
$\boldsymbol{\Delta}$ ... Mean Max-Relative Error compared to the exact result, i.e. $\frac{\langle |\boldsymbol{y}_{prediction} - \boldsymbol{y}_{exact}| \rangle}{\max |\boldsymbol{y}_{exact}|}$

Mode	**SecLevel**	$\boldsymbol{B_1}$	$\boldsymbol{B_2}$	$\boldsymbol{N}$	**MatMul**	$\boldsymbol{T}$ / s	$\boldsymbol{M}$ / MiB	$\boldsymbol{\Delta}$ / 1
Release	tc128	34	25	8192	Diagonal	8.39623	132.72	0.036462
					Hybrid	1.35514	132.72	0.0362841
					BSGS	1.66998	132.72	0.143365
	tc128	60	40	16384	Diagonal	17.2416	286.508	0.0363667
					Hybrid	3.05702	286.508	0.0364073
					BSGS	3.66647	286.508	0.139999
	tc256	60	40	32768	Diagonal	35.2401	615.163	0.036366
					Hybrid	5.99692	615.163	0.0364071
					BSGS	7.34914	615.163	0.139999
Debug	tc128	34	25	8192	Diagonal	7.80144	132.72	0.0358801
					Hybrid	1.33514	132.72	0.0370305
					BSGS	1.66876	132.72	0.143424

The above benchmarks (table 5.2) were accumulated on an Intel® i7-5600U CPU running at 2.6 GHz as the average over 3 individual runs with different test vectors, consistent accross different parameter runs.

Without any encryption, the neural network classifies the full 10,000 image dataset in 515 ms on the same machine, as compared to $3\frac{1}{2}$ hours for the encrypted evaluation.

Obviously, smaller parameters B_1, B_2, N yield smaller polynomials, in the number of coefficients as well as the coefficient representations, and therefore cause less computation and communication overhead. The slowest method is the diagonal method, followed by BSGS and the winner is the hybrid method in this case, though not by far in terms of speed! Looking at accuracy, the diagonal method wins, although it is negligibly close to the numeric accuracy of the hybrid method.

The most secure tested parameters are $60, 40, 32768$ which already lead to quite long classification times while ensuring a security level of 256 bits. For the web-based demonstrator (where speed matters), the natural choice is the first parameter set of $34, 25, 8192$ which allows for the most efficient computations and short response times in combination with the hybrid matrix multiplication method, while still guaranteeing 128-bit security.

5.4 Ciphertext Visualisations

In order to visually demonstrate the encryption, visualisations of the ciphertext polynomial c_0 (refer to section 3.4) were generated using a decomposition of the Residue Number System (RNS) representation of c_0. This is required because SEAL optimizes the storage of the ciphertext polynomials by splitting them up into sub-polynomials using the Chinese Remainder Theorem (CRT). The full modulus q, required to be huge for a secure system, is split up into multiple moduli $q_1, q_2, ...$, depending on the system parameters, so that $q = q_1 \cdot q_2 \cdot ... = \prod_{i=1} q_i$. Each pixel in the image below then corresponds to a coefficient $a \in \mathbb{Z}/q\mathbb{Z}$ scaled down by the total modulus q to obtain a brightness value between 0 and 1.

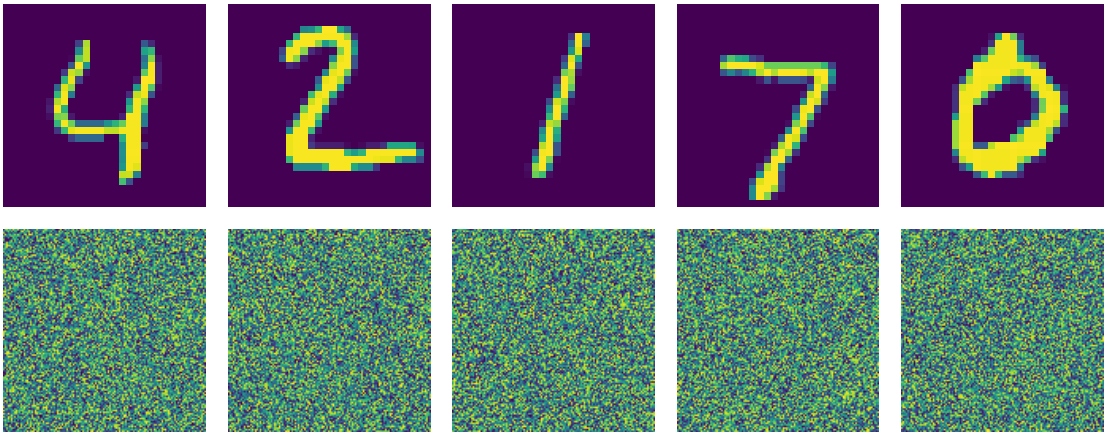

Figure 5.4: Ciphertext Visualisation: The first row corresponds to the images in plain, the second row depicts an encrypted version, namely the reconstructed polynomial coefficients a_k of the ciphertext polynomial.

Chapter 6

Conclusion

In the present thesis, we explored the interesting realm of homomorphic encryption in a machine-learning context while considering various security aspects of it. Next to the written part, the reader may find a server-client ('as a service') based demonstrator implementation of the homomorphically encrypted machine learning service for classifying handwritten digits, including a web-based frontend.

6.1 Summary

Chapter 2 introduced mathematical preliminaries of the lattice-based homomorphic encryptions schemes used in chapter 3. As the focus lies on thoroughly understanding the notation used in the encryption schemes, we first concentrated on the algebraic ring $\mathbb{Z}_q[X]/(X^N+1)$ with coefficients modulo q and the cyclotomic polynomial (X^N+1) as its modulus. Forming the basis of the upcoming cryptographic schemes, we introduced the LWE problem and its descendant, RLWE. The multi-layered neural network is trained using the backpropagation algorithm of the Tensorflow library, an approach similar to gradient descent - which was all introduced in the next section of chapter 2. The final section 2.4 introduced the reader to basic quantum mechanics and most of the necessary background to understand a simple quantum-mechanical system and the underlying principles of modern quantum computers.

Chapter 3 starts out with one of the first homomorphic schemes there is, unpadded RSA, motivating the need for a such structure. The first Fully Homomorphic Encryption scheme, invented by Craig Gentry in his PhD thesis, strongly inspired further developments in the field: Based on lattice problems and the RLWE cryptosystem, Brakerski; Fan and Vercauteren introduced the BFV scheme for integer arithmetic. Extending it, we arrived at CKKS scheme developed by Cheon et al. with an extensive encoding and decoding procedure. For both schemes, we verified the additive homomorphisms of the corresponding encryption (and encoding) operations BFV.Encrypt and CKKS.Encrypt $\circ$ CKKS.Encode.

Chapter 4 then presents details about the implementation of the web-based demonstrator, concerning the deployment and software architectural specifics. The focus however lies on the technical challenges with Homomorphic Encryption in practice. Four different matrix multiplication techniques were introduced in detail, gradually increasing the complexity but also the efficiency. The next challenge ahead was evaluating the activation function in between the two layers, due to technical reasons, only approximated by a series expansion. As we further

found in chapter 5, the most efficient multiplication method is the hybrid method. The results chapter presents the network's training results and a detailed statistical analysis of the network performance. To explicitly show the 'garbling' property of the encryption, the first polynomial of the ciphertext is visualised for a few test samples (figure 5.4). Finally, we analysed the runtime, network communication and numerical performance of the algorithms for different parameters, summarised in table 5.2.

Two longer proofs were outhoused to the Appendix A, one on the power-of-2 cyclotomic polynomials and a second one on the BSGS matrix multiplication method.

6.2 Related Works and Outlook

There are many existing approaches of PPML schemes or structures and even more applications - some related publications are, for the curious reader:

- CryptoNets (inferred ML), confer Dowlin et al. 2016.
- Gazelle (inferred ML) as described by Juvekar, Vaikuntanathan and Chandrakasan 2018.
- TFHE neural network inference, confer Chillotti et al. 2019.
- Random Forests using HE as described by Huynh 2020.
- Pasta for hybrid homomorphic encryption as described in Dobraunig et al. 2021.

Next to Microsoft SEAL, there are also other existing libraries for HE:

- Microsoft's PyEVA, an interface to SEAL's CKKS implementation.
- Halevi & Shoup's HELib, a separate implementation of HE algorithms using NTL (the number theoretic library).
- Palisade, another collection of many implemented HE algorithms, supposed to be a general-purpose tool.
- TenSEAL from OpenMined, a high-level Python interface to SEAL.
- PyGrid and PySyft from OpenMined, libraries to publish encrypted learning data (PyGrid) and utilize it (PySyft) for ML.

Considering the implications of mass surveilance and the thereby growing mindset for data privacy, the relevance of privacy-preserving/enhancing technologies will definitely grow in the coming years. The relatively new class of lattice cryptosystems looks immensely promising, given the interesting, especially useful properties of many such systems, and their inherent quantum security that will become even more relevant in the near future.

Acronyms, Definitions and Theorems

BFV	Brakerski-Fan-Vercauteren	2, 5
BGV	Brakerski-Gentry-Vaikuntanathan	5
BSGS	Babystep-Giantstep	44
CKKS	Cheon-Kim-Kim-Song	2, 5
CRT	Chinese Remainder Theorem	50
DFT	Discrete Fourier Transform	30
FFT	Fast Fourier Transform	30
FHE	Fully Homomorphic Encryption	5, 25
FHEW	Fastest Homomorphic Encryption in the West	25
GapSVP	Decisional Approximate Shortest Vector Problem	14
GD	Gradient Descent	18
HE	Homomorphic Encryption	6
iff	if and only if	9
LWE	Learning With Errors	2, 13
ML	Machine Learning	7, 17
MNIST	Modified National Institute of Standards and Technology	6, 37
MSE	Mean-Squared-Error	17
NP	Non-deterministic Polynomial time	5
PPML	Privacy-Preserving Machine Learning	2
QFT	Quantum Fourier Transform	24
RLWE	Learning With Errors on Rings	13
RNS	Residue Number System	50
RSA	Rivest-Shamir-Adleman	5
SEAL	Simple Encrypted Arithmetic Library	2, 6
SIMD	Single Instruction Multiple Data	41
SIS	Shortest Integer Solution	14
TFHE	Torus Fully Homomorphic Encryption	25
TLS	Transport Layer Security	15

Definitions

Theorems

Corollaries

Lemmata

Remarks

Bibliography

Ajtai, Miklós (1996). 'Generating hard instances of lattice problems'. In: *STOC '96*.

Bell, John Stewart, Michael A. Horne and Anton Zeilinger (1989). 'Speakable and Unspeakable in Quantum Mechanics'. In: *American Journal of Physics* 57, pp. 567–567.

Bishop, Christopher M. and Nasser M. Nasrabadi (2007). *Pattern Recognition and Machine Learning*. Vol. 16, p. 049901.

Brakerski, Zvika (2012). 'Fully Homomorphic Encryption without Modulus Switching from Classical GapSVP'. In: *IACR Cryptol. ePrint Arch.* 2012, p. 78. URL: https://link.springer.com/content/pdf/10.1007%2F978-3-642-32009-5_50.pdf.

Brakerski, Zvika, Craig Gentry and Vinod Vaikuntanathan (2012). '(Leveled) fully homomorphic encryption without bootstrapping'. In: *ITCS '12*.

Cheon, Jung Hee, Andrey Kim, Miran Kim and Yongsoo Song (2017). 'Homomorphic Encryption for Arithmetic of Approximate Numbers'. In: *ASIACRYPT*.

Chillotti, Ilaria, Nicolas Gama, Mariya Georgieva and Malika Izabachène (2019). 'TFHE: Fast Fully Homomorphic Encryption Over the Torus'. In: *Journal of Cryptology* 33, pp. 34–91.

Coppersmith, Don (1994). 'An approximate Fourier transform useful in quantum factoring'. In.

Corrigan-Gibbs, Henry, Sam Kim and David J. Wu (2018). *Lecture 9: Lattice Cryptography and the SIS Problem*. URL: https://crypto.stanford.edu/cs355/18sp/lec9.pdf (visited on 04/06/2022).

Dai, Wei (18th June 2020). *Multiply plain repeatedly and scale out of bound error*. URL: https://github.com/microsoft/SEAL/issues/182%5C#issuecomment-646234787 (visited on 20/04/2022).

Dobraunig, Christoph, Lorenzo Grassi, Lukas Helminger, Christian Rechberger, Markus Schofnegger and Roman Walch (2021). 'Pasta: A Case for Hybrid Homomorphic Encryption'. In: *IACR Cryptol. ePrint Arch.* 2021, p. 731.

Dowlin, Nathan, Ran Gilad-Bachrach, Kim Laine, Kristin Lauter, Michael Naehrig and John Wernsing (Feb. 2016). 'CryptoNets: Applying Neural Networks to Encrypted Data with High Throughput and Accuracy'. In: MSR-TR-2016-3. URL: https://www.microsoft.com/en-us/research/publication/cryptonets-applying-neural-networks-to-encrypted-data-with-high-throughput-and-accuracy/.

Ducas, Léo and Daniele Micciancio (2015). 'FHEW: Bootstrapping Homomorphic Encryption in Less Than a Second'. In: *EUROCRYPT*.

Fan, Junfeng and Frederik Vercauteren (2012). 'Somewhat Practical Fully Homomorphic Encryption'. In: https://eprint.iacr.org/2012/144. URL: https://eprint.iacr.org/2012/144.

Gentry, Craig (2009). 'Fully homomorphic encryption using ideal lattices'. In: *STOC '09*.

Goldwasser, Shafi (2018). 'From Idea to Impact, the Crypto Story: What's Next?' In: URL: https://www.youtube.com/watch?v=culuNbMPP0k (visited on 01/03/2022).

Grover, Lov K. (1996). *A fast quantum mechanical algorithm for database search*. DOI: 10.48550/ARXIV.QUANT-PH/9605043. URL: https://arxiv.org/abs/quant-ph/9605043.

Halevi, Shai and Victor Shoup (2018). *Faster Homomorphic Linear Transformations in HElib*. Cryptology ePrint Archive, Report 2018/244. https://ia.cr/2018/244.

Hornik, Kurt, Maxwell B. Stinchcombe and Halbert L. White (1989). 'Multilayer feedforward networks are universal approximators'. In: *Neural Networks* 2, pp. 359–366.

Huynh, Daniel (2020). 'Cryptotree: fast and accurate predictions on encrypted structured data'. In: DOI: 10.48550/ARXIV.2006.08299. URL: https://arxiv.org/abs/2006.08299.

Juvekar, Chiraag, Vinod Vaikuntanathan and Anantha P. Chandrakasan (2018). 'Gazelle: A Low Latency Framework for Secure Neural Network Inference'. In: *CoRR* abs/1801.05507. arXiv: 1801.05507. URL: http://arxiv.org/abs/1801.05507.

Kim, Andrey, Yuriy Polyakov and Vincent Zucca (2021). *Revisiting Homomorphic Encryption Schemes for Finite Fields*. Cryptology ePrint Archive, Paper 2021/204. https://eprint.iacr.org/2021/204. URL: https://eprint.iacr.org/2021/204.

Laine, Kim (2020). *Result Ciphertext is Transparent*. GitHub. URL: https://github.com/microsoft/SEAL/issues/224#issuecomment-702516479 (visited on 04/03/2022).

LeCun, Yann and Corinna Cortes (1998). *The MNIST database of handwritten digits*. URL: http://yann.lecun.com/exdb/mnist/.

Lepoint, Tancrède and Michael Naehrig (2014). 'A Comparison of the Homomorphic Encryption Schemes FV and YASHE'. In: *AFRICACRYPT*.

Lyubashevsky, Vadim, Chris Peikert and Oded Regev (2010). 'On Ideal Lattices and Learning with Errors over Rings'. In: *EUROCRYPT*.

– (2013). 'A Toolkit for Ring-LWE Cryptography'. In: *IACR Cryptol. ePrint Arch.*

Mackay, David J. C. (2004). 'Information Theory, Inference, and Learning Algorithms'. In: *IEEE Transactions on Information Theory* 50, pp. 2544–2545. URL: http://www.inference.org.uk/itprnn/book.pdf (visited on 17/07/2022).

Micciancio, Daniele (2010). 'A first glimpse of cryptography's Holy Grail'. In: *Commun. ACM* 53, p. 96.

Nüst, Daniel, Vanessa Sochat, Ben Marwick, Stephen J. Eglen, Tim Head, Tony Hirst and Benjamin D. Evans (2020). 'Ten simple rules for writing Dockerfiles for reproducible data science'. In: *PLOS Computational Biology* 16.11, e1008316. DOI: 10.1371/journal.pcbi.1008316.

Peikert, Chris (2016). 'A Decade of Lattice Cryptography'. In: *IACR Cryptol. ePrint Arch.* 2015, p. 939.

ProofWiki (2020). *Cyclotomic Polynomial of Index Power of Two*. URL: https://proofwiki.org/wiki/Cyclotomic_Polynomial_of_Index_Power_of_Two (visited on 06/06/2022).

Regev, Oded (2005). 'On lattices, learning with errors, random linear codes, and cryptography'. In: *STOC '05*.

– (2010). 'The learning with errors problem'. English (US). In: *Proceedings - 25th Annual IEEE Conference on Computational Complexity, CCC 2010*. Proceedings of the Annual IEEE

Conference on Computational Complexity. 25th Annual IEEE Conference on Computational Complexity, CCC 2010 ; Conference date: 09-06-2010 Through 11-06-2010, pp. 191–204. ISBN: 9780769540603. DOI: 10.1109/CCC.2010.26.

Rescorla, Eric (2018). *The Transport Layer Security (TLS) Protocol Version 1.3*. RFC 8446. DOI: 10.17487/RFC8446. URL: https://www.rfc-editor.org/info/rfc8446.

Rivest, Ronald, Leonard Adleman and Michael Dertouzos (1978). 'On Data Banks And Privacy Homomorphisms'. In.

Rivest, Ronald L, Adi Shamir and Leonard M Adleman (Sept. 1983). *Cryptographic communications system and method*. US Patent 4,405,829.

Microsoft SEAL 4.0 (Mar. 2022). https://github.com/Microsoft/SEAL. Microsoft Research, Redmond, WA.

Serge, Lang (2002). *Algebra*. 3rd ed. Springer. DOI: 10.1007/978-1-4613-0041-0.

Shor, Peter W. (Oct. 1997). 'Polynomial-Time Algorithms for Prime Factorization and Discrete Logarithms on a Quantum Computer'. In: *SIAM Journal on Computing* 26.5, pp. 1484–1509. DOI: 10.1137/s0097539795293172.

StackExchange (2020). *Plot gradient descent*. user194703. URL: https://tex.stackexchange.com/a/544832/155678 (visited on 07/07/2022).

Yin, Juan, Yuan Cao, Hai-Lin Yong, Ji-Gang Ren, Hao Liang, Sheng-Kai Liao, Fei Zhou, Chang Liu, Yu-Ping Wu, Ge-Sheng Pan, Li Li, Nai-Le Liu, Qiang Zhang, Cheng-Zhi Peng and Jian-Wei Pan (June 2013). 'Lower Bound on the Speed of Nonlocal Correlations without Locality and Measurement Choice Loopholes'. In: *Physical Review Letters* 110.26. DOI: 10.1103/physrevlett.110.260407. URL: https://doi.org/10.1103%2Fphysrevlett.110.260407.

List of Figures

List of Tables

Appendix A – Supplemental Proofs

A.1 Power-of-2 Cyclotomic Polynomials

Proof of theorem 2.1.1. With $k \in \mathbb{N}$ a positive integer, we want to show that

$$\Phi_{2^k}(x) = x^{2^{k-1}} + 1\,.$$

A polynomial $p \in \mathbb{Z}[X]$ with

$$p(x) = x^n - a$$

of degree n has n roots

$$\{x_j\} = \{a^{\frac{1}{n}} e^{2\pi i \frac{j}{n}} \,|\, j \in \mathbb{N}, j \leq n\}$$

related by a factor $a^{\frac{1}{n}}$ to the n^{th} roots of unity given by powers of $\xi = e^{2\pi i \frac{1}{n}}$.

It is clear from the fundamental theorem of algebra that the polynomial p with roots $\{x_j\}$ can be factorised as

$$p(x) = \prod_{j=1}^{n}(x - x_j) = \prod_{j=1}^{n}(x - a^{\frac{1}{n}} e^{2\pi i \frac{j}{n}})\,.$$

Fixing $a = -1$, we obtain $p(x) = x^n + 1$ with roots given by

$$x_j = (-1)^{\frac{1}{n}} e^{2\pi i \frac{j}{n}} = (e^{i\pi})^{\frac{1}{n}} e^{2\pi i \frac{j}{n}} = e^{\frac{i\pi(2j+1)}{n}}$$

and according factorisation

$$p(x) = \prod_{j=1}^{n}(x - e^{\frac{i\pi}{n}(2j+1)})\,.$$

Further letting $n = 2^{k-1}$ and observing that

$$\gcd(2^k, l) = \begin{cases} 1 & \text{if } l \text{ odd} \\ 2 & \text{if } l \text{ even} \end{cases} \qquad l, k \in \mathbb{N}$$

since a number 2^k that can only be decomposed into multiples of 2 never shares a factor with an odd number, in accordance with lemma 2.1.2 we can conclude that the set of all odd roots of unity is exactly the set of all primitive roots (satisfying $\gcd(2^k, l) = 1$).

Following from above,

$$p(x) = \prod_{j=1}^{2^{k-1}}(x - e^{\frac{i\pi}{n}(2j+1)}) = \prod_{\substack{l=1 \\ l \text{ odd}}}^{2^k}(x - e^{\frac{i\pi}{n}l}) = \prod_{\substack{l=1 \\ \xi^l \text{ primitive}}}^{2^k}(x - \xi^l) = \Phi_{2^k}(x)$$

we arrive exactly at the definition of a cyclotomic polynomial (definition 2.1.5).
(ProofWiki 2020) □

A.2 Babystep-Giantstep Multiplication

Proof of theorem 4.4.3. Starting from the adapted BSGS matrix-multiplication result $P = (P_1, P_2, ..., P_t)^T \in \mathbb{R}^t$, we want to show that we indeed end up with an authentic matrix-vector product.

$$P_i := \left\{ \sum_{k=0}^{t_2-1} \mathrm{rot}_{(kt_1)}\Big(\sum_{j=0}^{t_1-1} \mathrm{diag}'_{(kt_1+j)}(M) \cdot \mathrm{rot}_j(\boldsymbol{x}) \Big) \right\}_i = \sum_{k=0}^{t_2-1} \sum_{j=0}^{t_1-1} m'_{kt_1+j,(i+kt_1)} x_{(i+kt_1)+j}$$

with

$$m'_{p,i} = \Big\{ \mathrm{diag}'_p(M) \Big\}_i = \Big\{ \mathrm{rot}_{-\lfloor p/t_1 \rfloor \cdot t_1}(\mathrm{diag}_p(M)) \Big\}_i = M_{i-\lfloor \frac{p}{t_1} \rfloor t_1, i-\lfloor \frac{p}{t_1} \rfloor t_1 + p}$$

and therefore

$$\begin{aligned} m'_{kt_1+j,i} &= M_{i-\lfloor \frac{kt_1+j}{t_1} \rfloor t_1, i-\lfloor \frac{kt_1+j}{t_1} \rfloor t_1 + kt_1 + j} \\ &= M_{i-kt_1-\lfloor \frac{j}{t_1} \rfloor t_1, i-kt_1-\lfloor \frac{j}{t_1} \rfloor t_1 + kt_1 + j} \\ &= M_{i-kt_1-\lfloor \frac{j}{t_1} \rfloor t_1, i+j-\lfloor \frac{j}{t_1} \rfloor t_1} \\ m'_{kt_1+j,(i+kt_1)} &= M_{i+kt_1-kt_1-\lfloor \frac{j}{t_1} \rfloor t_1, i+kt_1+j-\lfloor \frac{j}{t_1} \rfloor t_1} \\ &= M_{i-\lfloor \frac{j}{t_1} \rfloor t_1, i+kt_1+j-\lfloor \frac{j}{t_1} \rfloor t_1} \end{aligned}$$

leading to

$$P_i = \sum_{k=0}^{t_2-1} \sum_{j=0}^{t_1-1} m'_{kt_1+j,(i+kt_1)} x_{(i+kt_1)+j} = \sum_{k=0}^{t_2-1} \sum_{j=0}^{t_1-1} M_{i-\lfloor \frac{j}{t_1} \rfloor t_1, i+kt_1+j-\lfloor \frac{j}{t_1} \rfloor t_1} x_{(i+kt_1)+j} \,.$$

Noticing that the downward rounded fraction $\lfloor \frac{j}{t_1} \rfloor$ vanishes in a sum with j running from 0 to $t_1 - 1$, we can simplify to

$$P_i = \sum_{k=0}^{t_2-1} \sum_{j=0}^{t_1-1} M_{i,i+kt_1+j} x_{i+kt_1+j}$$

which contains two sums running to t_1 and t_2 respectively, containing an expression of the form $k \cdot t_1 + j$, which allows us to condense the nested sums into one single summation expression, as

$$\sum_{k=0}^{t_2-1} \sum_{j=0}^{t_1-1} f(kt_1 + j) = \sum_{l=0}^{t-1} f(l)$$

indeed catches every single value $l \in \{0, 1, 2, ..., t = t_1 \cdot t_2\}$ with $l = kt_1 + j$.
In summary, we obtain

$$\begin{aligned} P_i &= \sum_{k=0}^{t_2-1} \sum_{j=0}^{t_1-1} M_{i,i+kt_1+j} x_{i+kt_1+j} \\ &= \sum_{l=0}^{t-1} M_{i,i+l} x_{i+l} = \sum_{\nu=0}^{t-1} M_{i,\nu} x_\nu \\ &= \Big\{ M\boldsymbol{x} \Big\}_i \end{aligned}$$

which indeed equals the conventional definition of a matrix-vector product. □